Title

Cofactor Selectivity in Methylmalonyl Coenzyme A Mutase, a Model Cobamide-Dependent Enzyme

Permalink

Journal

ISSN

Authors

Sokolovskaya, Olga M
Mok, Kenny C
Park, Jong Duk
et al.

Publication Date

DOI

Peer reviewed

Cofactor Selectivity in Methylmalonyl Coenzyme A Mutase, a Model Cobamide-Dependent Enzyme

Olga M. Sokolovskaya,[a,b] Kenny C. Mok,[a] Jong Duk Park,[a*] Jennifer L. A. Tran,[a*] Kathryn A. Quanstrom,[a*] Michiko E. Taga[a]

[a]Department of Plant & Microbial Biology, University of California Berkeley, Berkeley, California, USA
[b]Department of Chemistry, University of California Berkeley, Berkeley, California, USA

ABSTRACT Cobamides, a uniquely diverse family of enzyme cofactors related to vitamin B_{12}, are produced exclusively by bacteria and archaea but used in all domains of life. While it is widely accepted that cobamide-dependent organisms require specific cobamides for their metabolism, the biochemical mechanisms that make cobamides functionally distinct are largely unknown. Here, we examine the effects of cobamide structural variation on a model cobamide-dependent enzyme, methylmalonyl coenzyme A (CoA) mutase (MCM). The *in vitro* binding affinity of MCM for cobamides can be dramatically influenced by small changes in the structure of the lower ligand of the cobamide, and binding selectivity differs between bacterial orthologs of MCM. In contrast, variations in the lower ligand have minor effects on MCM catalysis. Bacterial growth assays demonstrate that cobamide requirements of MCM *in vitro* largely correlate with *in vivo* cobamide dependence. This result underscores the importance of enzyme selectivity in the cobamide-dependent physiology of bacteria.

IMPORTANCE Cobamides, including vitamin B_{12}, are enzyme cofactors used by organisms in all domains of life. Cobamides are structurally diverse, and microbial growth and metabolism vary based on cobamide structure. Understanding cobamide preference in microorganisms is important given that cobamides are widely used and appear to mediate microbial interactions in host-associated and aquatic environments. Until now, the biochemical basis for cobamide preferences was largely unknown. In this study, we analyzed the effects of the structural diversity of cobamides on a model cobamide-dependent enzyme, methylmalonyl-CoA mutase (MCM). We found that very small changes in cobamide structure could dramatically affect the binding affinity of cobamides to MCM. Strikingly, cobamide-dependent growth of a model bacterium, *Sinorhizobium meliloti*, largely correlated with the cofactor binding selectivity of *S. meliloti* MCM, emphasizing the importance of cobamide-dependent enzyme selectivity in bacterial growth and cobamide-mediated microbial interactions.

KEYWORDS *Sinorhizobium meliloti*, chemical diversity, cobalamin, cobamides, enzyme selectivity

Cobalamin, commonly referred to as vitamin B_{12}, is a versatile enzyme cofactor used by organisms in all domains of life. In humans, cobalamin is essential for methionine synthesis and the breakdown of fatty acids, amino acids, and cholesterol (1, 2). Bacteria and archaea additionally use cobalamin and related cofactors, cobamides, for deoxyribonucleotide synthesis (3), metabolism of various carbon and energy sources (4–17), synthesis of secondary metabolites (18–25), sensing light (26), and other processes (15–17, 27–32). The finding that 86% of bacterial species encode at least one cobamide-dependent enzyme in their genome (33) demonstrates the prevalence of cobamide-dependent metabolisms. Widespread use of these cofactors can be attrib-

R = 5'-deoxyadenosine, methyl,
cyanide, water

FIG 1 The structure of cobalamin. The lower ligand, boxed, varies in other cobamides. Cobinamide, a cobamide precursor, lacks a nucleotide base (delineated by the wavy line).

uted to their chemical versatility, as they facilitate challenging chemical reactions, including radical-initiated rearrangements, methylation reactions, and reductive cleavage of chemical bonds (34, 35).

All cobamides share the same core structure (Fig. 1): a corrin ring that coordinates a cobalt ion, a variable "upper" axial ligand (*R* in Fig. 1), and a pseudonucleotide that is covalently attached to the corrin ring through an aminopropanol linker (36) or an ethanolamine linker, in the case of norcobamides (37, 38). The major differences among cobamides are in the structure of the nucleotide base, more commonly referred to as the lower axial ligand for its ability to coordinate the central cobalt ion. In cobalamin, the lower ligand is 5,6-dimethylbenzimidazole (Fig. 1, boxed); in other naturally occurring cobamides, different benzimidazoles, phenolics, and purines constitute the lower ligand (Table 1 and Fig. 2C) (39–43). Phenolyl cobamides are distinct in that they lack the coordinate bond between the lower ligand and cobalt ion.

While cobamides containing different lower ligands share the same chemically

TABLE 1 Abbreviations used for cobamides and upper axial ligands

Abbreviation or prefix	Cobamide name or upper ligand
Abbreviation	
Cbl	Cobalamin
[5-MeBza]Cba	5-Methylbenzimidazolylcobamide
[Bza]Cba	Benzimidazolylcobamide
[5-OHBza]Cba	5-Hydroxybenzimidazolylcobamide
[Cre]Cba	*para*-Cresolylcobamide
[Phe]Cba	Phenolylcobamide
[Ade]Cba	Adeninylcobamide
[2-MeAde]Cba	2-Methyladeninylcobamide
[Pur]Cba	Purinylcobamide
[7-MeBza]Cba	7-Methylbenzimidazolylcobamide
[7-AmBza]Cba	7-Aminobenzimidazolylcobamide
[6-AzaBza]Cba	6-Azabenzimidazolylcobamide
[3-DeazaAde]Cba	3-Deazaadeninylcobamide
[6-MePur]Cba	6-Methylpurinylcobamide
Prefix	
Ado	5'-Deoxyadenosine
CN	Cyanide
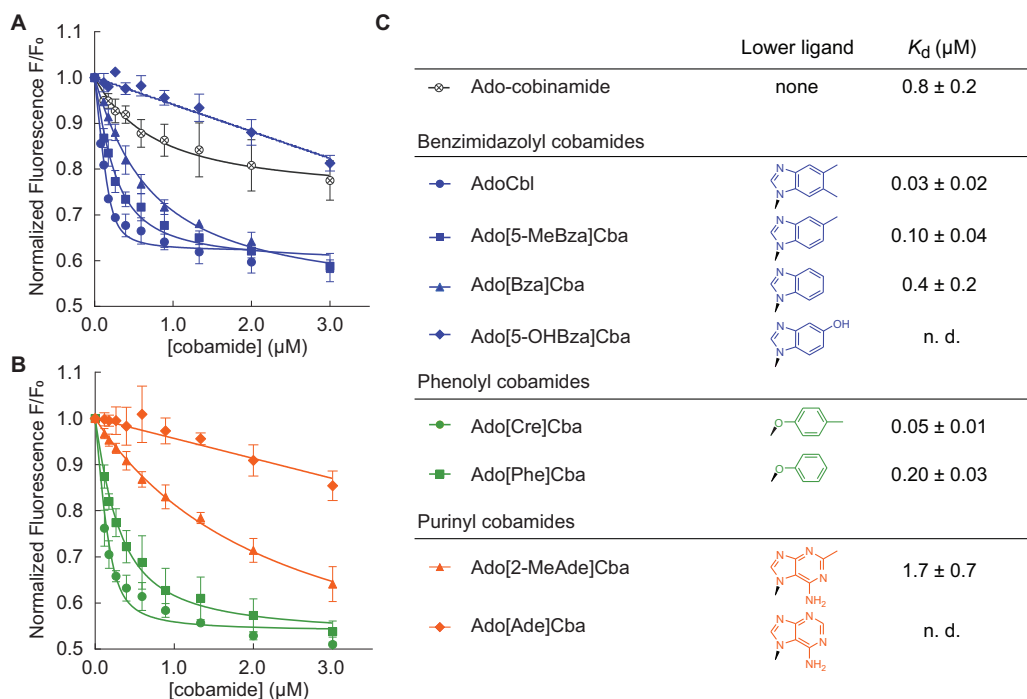
FIG 2 Binding of diverse cobamides to SmMCM (see also Fig. S1). (A and B) Fluorescence decrease of SmMCM when reconstituted with benzimidazolyl cobamides (blue), cobinamide (black), phenolyl cobamides (green), and purinyl cobamides (orange). Data points represent the mean and standard deviation for three technical replicates from a single experiment. (C) K_d values for different cobamides, reported as the average and standard deviation for three or more independent experiments, each consisting of technical triplicates. "n. d.," not determined, indicating that binding was too weak to determine K_d.

reactive moieties, specifically the cobalt center and methyl or 5'-deoxyadenosyl upper axial ligands, they are nonetheless functionally distinct. Culture-based studies have shown that only a subset of cobamides supports a given bacterial metabolism, and uptake or production of other cobamides can inhibit growth (39, 44–49). The requirements of bacteria for particular cobamides are notable given the diversity of cobamides present in host-associated and environmental samples (40–42), coupled with the absence of de novo cobamide biosynthesis in more than half of bacteria (33). Despite the biological relevance of cobamide structure, and the prevalence of cobamide use among bacteria (33, 50–52), little is understood about the biochemical mechanisms by which cobamides differentially impact microbial physiology.

The effect of lower ligand structure on the biochemistry of cobamide-dependent enzymes has been studied to a limited extent. In "base-on" enzymes, the lower ligand base coordinates the central cobalt ion of the cobamide, as drawn in Fig. 1 (53–55). Because the lower ligand is part of the catalytic center of the enzyme, lower ligand structure can influence catalysis through a variety of mechanisms (56–58), and cobamides unable to form an intramolecular coordinate bond are catalytically inactive in base-on enzymes (59, 60). In contrast, in "base-off" enzymes the lower ligand is bound by the enzyme more than 10 Å away from the active site (20, 61–70). In a subset of base-off enzymes, referred to as "base-off/His-on," a histidine residue from the protein coordinates the cobalt ion in place of the lower ligand (61, 63). Despite its distance from the reactive center, lower ligand structure affects the activity of base-off enzymes, as evidenced by the cobamide cofactor selectivity of methionine synthase (71), methylmalonyl coenzyme A (CoA) mutase (MCM) (60, 72), reductive dehalogenases (49), and other enzymes (59, 72, 73). However, the mechanisms by which lower ligand structure affects the biochemistry of base-off cobamide-dependent enzymes remain unclear.

As MCM is one of the most abundant cobamide-dependent enzymes in bacterial

genomes (33), and one of the two cobamide-dependent enzymes in humans, we have chosen to study the cobamide selectivity of MCM as a model for base-off/His-on enzymes, all of which share a structurally conserved B_{12}-binding domain (63, 74). MCM catalyzes the interconversion of (R)-methylmalonyl-CoA and succinyl-CoA, a bidirectional reaction used in propionate metabolism (12, 75, 76), catabolism of branched amino acids and odd-chain fatty acids (76, 77), polyhydroxybutyrate degradation (78), secondary metabolite biosynthesis (79), and autotrophic carbon dioxide fixation (4, 80). MCM-dependent pathways have been harnessed industrially for the bioproduction of propionate, bioplastics, biofuels, and antibiotics (81–88).

The presence of a cobamide lower ligand is required for MCM activity, as evidenced by the observation that adenosylcobinamide, a cobamide intermediate lacking a lower ligand (Fig. 1), does not support MCM activity *in vitro* (89). Three studies provide evidence that MCM is selective for cobamides with particular lower ligands. First, MCM from *Propionibacterium shermanii* was found to have different apparent K_m values for cobamides, increasing from AdoCbl to Ado[Bza]Cba to Ado[Ade]Cba (refer to Table 1 for full names of cobamides), and MCM from sheep had a higher apparent K_m for Ado[Bza]Cba than AdoCbl (72). Second, *P. shermanii* MCM had a lower apparent K_m for Ado[Cre]Cba than AdoCbl (60). Third, in *Sinorhizobium meliloti* bacteroids, MCM activity was highest with AdoCbl, intermediate with Ado[Bza]Cba, and absent with Ado[Ade]Cba (90). Each of these studies includes only one or two cobamides other than cobalamin, and understandably so; cobamides are difficult to obtain in high quantities and must be purified from large volumes of bacterial cultures. Because of this, the response of MCM orthologs to the full diversity of cobamides has not been explored, and the mechanistic basis of cobamide selectivity remains unclear.

To investigate the mechanisms by which diverse lower ligands affect MCM function, we conducted *in vitro* binding and activity assays with MCM from *S. meliloti* (*Sm*MCM). We discovered major differences in the binding affinities of eight naturally occurring cobamides for *Sm*MCM, while cobamide structure affected enzyme activity to a lesser extent. Using six additional cobamides, five of which are novel analogs that have not been observed in nature or described previously, we identified structural elements of lower ligands that are determinants of binding to *Sm*MCM. To probe the hypothesis that enzyme selectivity influences bacterial growth, we characterized the cobamide dependence of *S. meliloti* growth *in vivo*. By bridging the results of *in vitro* biochemistry of three bacterial MCM orthologs and the cobamide-dependent growth phenotypes of *S. meliloti*, we have elucidated molecular factors that contribute to the cobamide-dependent physiology of bacteria.

RESULTS

Lower ligand structure influences cobamide binding to MCM. We chose *Sm*MCM as a model to examine how lower ligand structure influences MCM function based on previous work demonstrating its activity as a homodimer encoded by a single gene (91, 92). We purified eight naturally occurring cobamides for *in vitro* studies of this protein and chemically adenosylated each cobamide to produce the biologically active form used by MCM for catalysis. Previous studies showed that binding of cobamides to *P. shermanii* MCM can be detected *in vitro* by measuring quenching of intrinsic protein fluorescence (89). We found that the fluorescence of purified, His-tagged *Sm*MCM also decreased in a dose-dependent manner when the protein was reconstituted with increasing concentrations of AdoCbl (Fig. 2A). The equilibrium dissociation constant (K_d) derived from these measurements, $0.03 \pm 0.02 \mu M$ (Fig. 2C), is 6-fold lower than the K_d reported for *P. shermanii* MCM (89). Adocobinamide also bound *Sm*MCM, as was observed with *P. shermanii* MCM (89), albeit with over 10-fold-reduced affinity compared to cobalamin (Fig. 2A and C).

We next measured binding of other benzimidazolyl cobamides to *Sm*MCM and found that Ado[5-MeBza]Cba and Ado[Bza]Cba, the cobamides most structurally similar to AdoCbl, also bound the enzyme. However, the absence of one or two methyl groups,
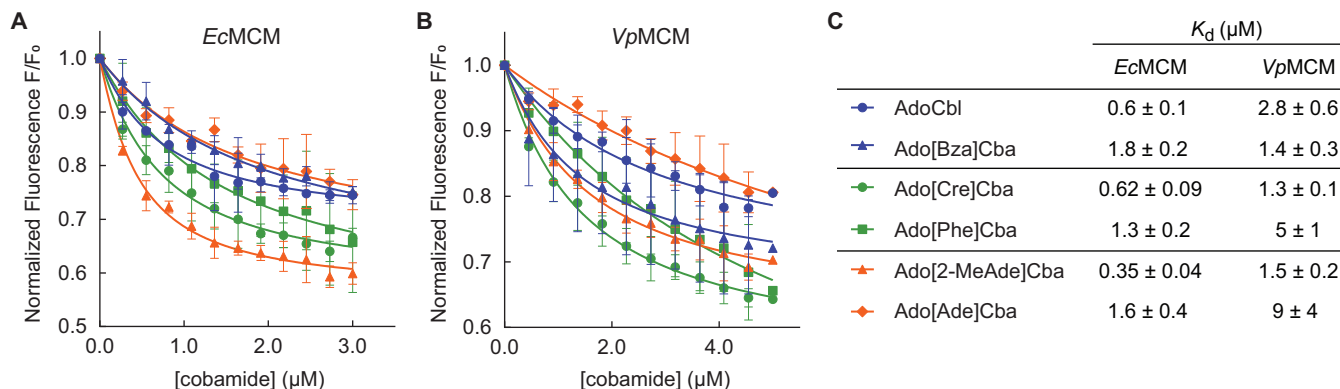
FIG 3 Binding selectivity of diverse MCM orthologs (see also Fig. S2). Fluorescence binding assays with *E. coli* MCM (A) and *V. parvula* MCM (B). Data points and error bars represent the mean and standard deviation, respectively, for technical triplicates from a single experiment; each replicate consisted of an independent cobamide dilution. K_d values from the fitted curves in panels A and B are reported in panel C; error values reflect the standard error of the curve fit. K_d values for *Vp*MCM binding to Ado[Cre]Cba and AdoCbl and for *Ec*MCM binding to all cobamides were reproduced in independent experiments.

respectively, in the lower ligands of these cobamides caused a decrease in binding affinity relative to AdoCbl (Fig. 2A and C). Strikingly, no binding of Ado[5-OHBza]Cba to *Sm*MCM was detected at low-micromolar concentrations. To rule out the possibility that Ado[5-OHBza]Cba binds *Sm*MCM but does not cause a fluorescence quench, we used an alternative, filtration-based, binding assay and observed little to no binding of Ado[5-OHBza]Cba to *Sm*MCM at micromolar concentrations (see Fig. S1A and B in the supplemental material).

We expanded our analysis of *Sm*MCM-cobamide binding selectivity to include cobamides from other structural classes. Both of the phenolyl cobamides tested, Ado[Cre]Cba and Ado[Phe]Cba, bound *Sm*MCM with affinities similar to those of cobalamin and other benzimidazolyl cobamides (Fig. 2B and C). In contrast, the purinyl cobamides Ado[2-MeAde]Cba and Ado[Ade]Cba had lower affinities for *Sm*MCM compared to most benzimidazolyl cobamides (Fig. 2B and C): Ado[2-MeAde]Cba bound *Sm*MCM with ~20-fold lower affinity than cobalamin, and Ado[Ade]Cba did not bind to any significant extent at micromolar concentrations (verified by the filtration assay [Fig. S1C]). Interestingly, for all three classes of lower ligands, the presence of a methyl substituent promoted binding relative to other cobamides of the same structural class.

Bacterial MCM orthologs have distinct selectivity. To test whether cofactor-binding selectivity is a general phenomenon across bacterial MCM orthologs, we compared the cobamide-binding profile of *Sm*MCM to that of MCM orthologs from *Escherichia coli* (*Ec*MCM) and *Veillonella parvula* (*Vp*MCM). Activity of *Ec*MCM with AdoCbl has been reported both *in vivo* and *in vitro*, although its physiological role in *E. coli* remains unclear (82, 93). Annotations for two MCM homologs are present in the genome of *V. parvula*, and we purified the one that exhibits MCM activity when expressed in *S. meliloti* (see Materials and Methods). Because *S. meliloti* produces cobalamin (94), *E. coli* produces [2-MeAde]Cba when provided with cobinamide (95), and *V. parvula* produces [Cre]Cba (96), we expected that each ortholog should have distinct cobamide selectivity. Indeed, *Ec*MCM had highest affinity for its native cobamide, Ado[2-MeAde]Cba (Fig. 3A and C). All other cobamides bound with 2- to 3-fold reduced affinities relative to Ado[2-MeAde]Cba. Similarly, *Vp*MCM had a higher affinity for Ado[Cre]Cba, its native cobamide, than AdoCbl (Fig. 3B and C). *Vp*MCM also bound Ado[2-MeAde]Cba and Ado[Bza]Cba with similar affinities. We observed differences between the total changes in fluorescence among cobamides with similar K_d values. This is not unexpected, as protein fluorescence is highly sensitive to local environment and may be affected by subtle conformational differences.

We constructed a sequence alignment of MCM orthologs from diverse organisms known to produce or use various cobamides, in search of amino acid residues that
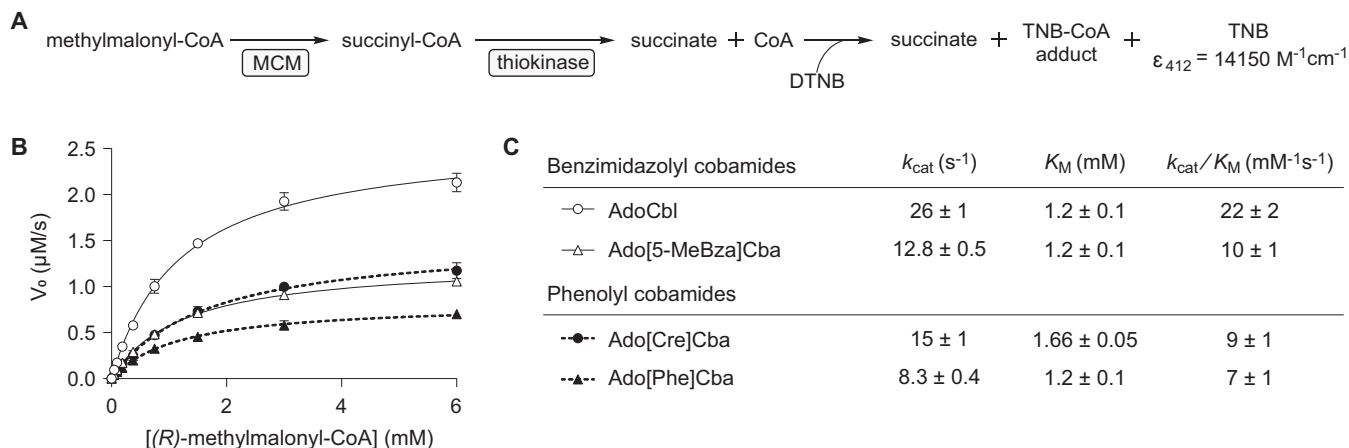
FIG 4 Activity of *Sinorhizobium meliloti* MCM with different cobamide cofactors. (A) Succinyl-CoA formation was detected using a coupled spectrophotometric assay (138). DTNB, dithionitrobenzoate (Ellman's reagent); TNB, thionitrobenzoate; CoA, coenzyme A. (B) Michaelis-Menten kinetic analysis of *Sm*MCM reconstituted with various cobamides. Data points and error bars represent the mean and standard deviation, respectively, for three technical replicates from one experiment; each replicate consisted of an independent substrate dilution. (C) Kinetic constants.

could account for differences in cobamide binding (Fig. S2A). The B_{12}-binding domains of diverse MCM orthologs had high overall amino acid identity (38 to 70%). Cases of low identity correlated with differences in the structural configuration of MCM, which occurs in different organisms as a homodimer (92, 93, 97, 98), heterodimer (61, 99–101), or heterotetramer (80, 102) (Fig. S2B). We focused our analysis on residues immediately surrounding the lower ligand in the available crystal structure of *Homo sapiens* MCM (97) (*Hs*MCM) (Fig. S2A, triangles). For the most part, these residues are highly conserved between orthologs. Interestingly, however, *Hs*MCM residues Phe638, Phe722, and Ala731, which are conserved in *Sm*MCM, are replaced with the more polar residues Tyr, Tyr, and Ser, respectively, in *Ec*MCM (Fig. S2A), which has a higher affinity for purinyl cobamides. Introducing mutations in *Sm*MCM and *Ec*MCM to test the importance of these residues proved challenging, as it resulted in reduced protein solubility and overall impaired cobamide binding (data not shown). Whether or not these residues covary with cobamide selectivity across other MCM orthologs is difficult to interpret because the cobamide selectivity of MCM from most organisms is unknown.

The lower ligand of cobamides modulates MCM reaction kinetics. We reconstituted *Sm*MCM with saturating amounts of each of the four cobamides that bound with highest affinity and measured conversion of (*R*)-methylmalonyl-CoA to succinyl-CoA under steady-state conditions. Interestingly, the substrate K_m was nearly invariable among the cobamides tested (Fig. 4). Turnover was highest with AdoCbl (26 ± 1 s^{-1}) and 2- to 3-fold lower with other cobamides. Thus, all of the cobamides tested supported *Sm*MCM catalysis with modest differences in k_{cat}. This finding is consistent with a previous observation that adenosylcobinamide-GDP, a cobamide precursor with an extended nucleotide loop and a guanine base, supported activity of *P. shermanii* MCM with only slight catalytic impairment compared to AdoCbl (103).

MCM-dependent growth of *S. meliloti* correlates with the binding selectivity of *Sm*MCM for benzimidazolyl and purinyl cobamides, but not phenolyl cobamides. To assess whether the cobamide-dependent growth of *S. meliloti* reflects MCM selectivity as observed *in vitro*, we cultured *S. meliloti* under conditions that require MCM activity. Examination of metabolic pathways encoded in the *S. meliloti* genome using the KEGG database (104) suggests that the degradation of branched amino acids isoleucine and valine to succinyl-CoA, an intermediate of the citric acid cycle, requires MCM. Indeed, growth of *S. meliloti* on L-isoleucine and L-valine as the only carbon sources was dependent on the presence of the *bhbA* gene, which encodes MCM (91) (Fig. S3).
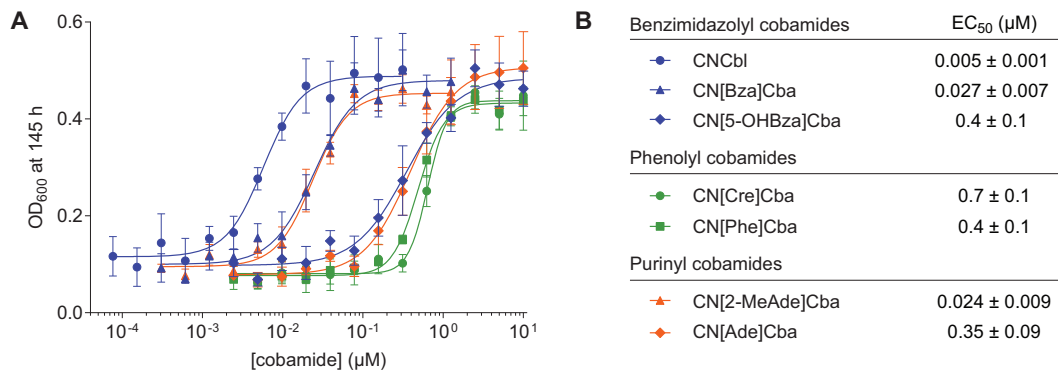
FIG 5 MCM-dependent growth of *S. meliloti cobD::gus* Gm^r *metH*::Tn*5* Δ*nrdJ* pMS03-*nrdAB$_{Ec}$*$^+$ with various cobamides (see also Fig. S3, S4, and S5). (A) Dose dependence of growth based on OD$_{600}$ at 145 h. Data points and error bars represent the mean and standard deviation, respectively, for three biological replicates from a single experiment. (B) EC$_{50}$ values are the average and standard deviation for five or more biological replicates across two or more independent experiments.

We constructed an *S. meliloti* strain incapable of synthesizing cobalamin and lacking cobamide-dependent enzymes other than MCM to ensure that differential growth could be attributed solely to MCM selectivity for added cobamides (see Materials and Methods). We cultivated this strain with L-isoleucine and L-valine as sole carbon sources in medium supplemented with different cobamides in their cyanylated (CN) form, which is the form typically used for *in vivo* growth assays. Under these growth conditions, the maximum growth yield (optical density at 600 nm [OD$_{600}$]) achieved at high concentrations of all of the cobamides was indistinguishable (Fig. S4A to G). However, the concentration of cobamides required to achieve half of the maximal OD$_{600}$ (50% effective concentration [EC$_{50}$]) differed based on the cobamide provided (Fig. 5). Consistent with the binding data, CNCbl had the lowest EC$_{50}$ value. EC$_{50}$ values for CN[Bza]Cba and CN[2-MeAde]Cba were 5-fold higher than CNCbl, and other cobamides had EC$_{50}$ values 2 orders of magnitude higher than CNCbl.

With the notable exception of the phenolyl cobamides, differences in the EC$_{50}$ values of cobamides *in vivo* qualitatively correlated with the binding selectivity that we observed *in vitro* (Fig. 2). Among benzimidazolyl cobamides, EC$_{50}$ values increased from cobalamin to [Bza]Cba to [5-OHBza]Cba, consistent with the relative binding affinities of these cobamides. Similarly, [2-MeAde]Cba, which had an intermediate binding affinity for *Sm*MCM, had a lower EC$_{50}$ value than [Ade]Cba, which did not bind to *Sm*MCM at low-micromolar concentrations *in vitro*. The ability of [5-OHBza]Cba and [Ade]Cba to support growth suggests that these cobamides can bind *Sm*MCM at concentrations higher than those tested *in vitro*; a control experiment with an *S. meliloti* strain lacking MCM rules out the possibility that high concentrations of cobamides (10 µM) abiotically enable growth on isoleucine and valine (Fig. S3).

We considered the possibility that differences in cobamide internalization by *S. meliloti* could also influence the EC$_{50}$ measurements shown in Fig. 5. When *S. meliloti* cultures were supplemented with equimolar amounts of CNCbl, CN[Ade]Cba, or CN-[Cre]Cba, the concentration of cobalamin extracted from the cellular fraction was 2- to 3-fold higher than [Ade]Cba and 5- to 6-fold higher than [Cre]Cba (Fig. S5A). This result suggests that cobamides are differentially internalized or retained by the cells. However, MCM-dependent growth does not correlate with intracellular cobamide concentrations, as intracellular concentrations of cobalamin comparable to those of [Ade]Cba and [Cre]Cba supported *S. meliloti* growth to high densities (Fig. S5). Therefore, the high EC$_{50}$ of CN[Ade]Cba relative to CNCbl is more likely attributable to enzyme selectivity. Additional factors that could explain the high EC$_{50}$ values of the phenolyl cobamides are considered in Discussion.

Identification of structural elements that interfere with cobamide binding. Given the apparent importance of MCM cobamide binding selectivity for the cobamide-
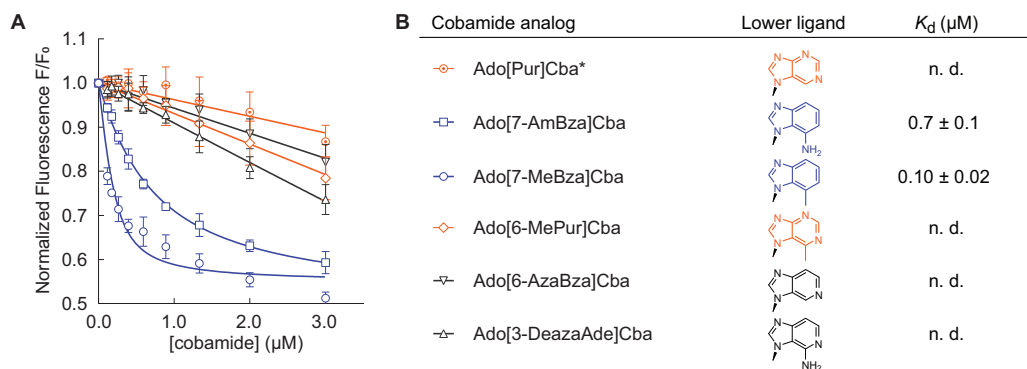
FIG 6 Binding of cobamide analogs to SmMCM (see also Fig. S8). (A) Fluorescence decrease of SmMCM when reconstituted with benzimidazolyl (blue), purinyl (orange), and azabenzimidazolyl (black) cobamide analogs. Data points represent the mean and standard deviation for three technical replicates from a single experiment. (B) K_d values for different cobamides, reported as the average and standard deviation for three or more independent experiments, each consisting of technical triplicates. "n. d.," not determined, indicating that binding was too weak to determine K_d. The asterisk indicates that, while it was unreported at the time of our study, [Pur]Cba was discovered to be the cobamide naturally produced by Desulfitobacterium hafniense (39).

dependent growth of *S. meliloti*, we pursued a more mechanistic understanding of how lower ligand structure affects cobamide binding. When cobamides are bound to MCM, the lower ligand is surrounded by protein residues (61, 97). Therefore, the reduced affinity of certain cobamides for the enzyme could be a result of exclusion of their lower ligands from this binding pocket because of steric or electrostatic repulsion. We hypothesized that the poor binding of the purinyl cobamides Ado[Ade]Cba and Ado[2-MeAde]Cba is due to the presence of the exocyclic amine based on several observations: (i) Ado[5-OHBza]Cba, which also contains a polar functional group, had impaired binding to SmMCM (Fig. 2A and C). (ii) In the crystal structure of HsMCM (97), residues Phe722 and Ala731, which are conserved in SmMCM, would be expected to electrostatically occlude the exocyclic amine of [Ade]Cba (Fig. S6A, asterisk). Based on sequence alignment (Fig. S2A), polar residues Tyr and Ser would be expected to occupy the corresponding positions in EcMCM, which has higher affinity for purinyl cobamides. (iii) Structural modeling of Ado[Ade]Cba bound to HsMCM, which shares 59% amino acid identity to SmMCM in the B_{12}-binding domain, suggests significant displacement of the adenine lower ligand relative to the lower ligand of AdoCbl, in the direction that would be consistent with steric or electrostatic repulsion of the exocyclic amine by surrounding residues (Fig. S6B to D).

To test the importance of the exocyclic amine of adenine in cofactor exclusion, we produced an unsubstituted purinyl cobamide, Ado[Pur]Cba (39). Ado[Pur]Cba also had low affinity for SmMCM (Fig. 6A and B), suggesting that the exocyclic amine of adenine is not a major cause of binding exclusion. Consistent with this result, a novel benzimidazolyl cobamide, Ado[7-AmBza]Cba, bound SmMCM with comparable affinity as Ado[Bza]Cba, despite being functionalized with an exocyclic amine (Fig. 6A and B). Rather, these results suggest that the presence of nitrogens in the six-membered ring of the lower ligand interferes with binding. To test this hypothesis directly, we produced three cobamide analogs with at least one nitrogen in the six-membered ring of the lower ligand base. Comparison of the binding of Ado[7-MeBza]Cba and Ado[6-MePur]Cba (Fig. 6A and B) supported a role of ring nitrogens in binding inhibition, and comparison of binding affinities between Ado[Bza]Cba and Ado[6-AzaBza]Cba (105) (Fig. 2A and C and Fig. 6A and B, respectively), and between Ado[7-AmBza]Cba and Ado[3-DeazaAde]Cba (Fig. 6A and B), revealed that a single nitrogen atom in the six-membered ring of the lower ligand was sufficient to severely impair binding.

As it was recently discovered to be a naturally occurring cobamide (39), we tested the MCM-dependent growth of *S. meliloti* with [Pur]Cba. [Pur]Cba had a high EC_{50} value of 0.6 ± 0.2 μM (Fig. S4H), further supporting the correlation between

binding and growth that we previously observed for benzimidazolyl and purinyl cobamides.

DISCUSSION

Cobamides are distinct from other cofactors in their extensive structural diversity, with over a dozen forms that differ in the lower ligand base and nucleotide loop. How cobamide lower ligand structure influences the activity of cobamide-dependent enzymes has not been extensively explored. Here, we report a systematic analysis of the effects of cobamide lower ligand structure on the function of a model cobamide-dependent enzyme, MCM. Our results show that MCM exhibits varied affinities for different cobamides and that this selectivity is linked to the physiology of the organism.

Our results show that the major determinant of cobamide selectivity in *Sm*MCM is binding, with small changes in the lower ligand capable of dramatically altering the binding affinity of a cobamide. One explanation for these differences is that the chemical compatibility between the lower ligand base and the binding pocket of the protein strongly influences the binding affinity of cobamides; repulsion of the lower ligand on the basis of electrostatics could reduce the binding affinity of cobamides to MCM. While the structure of *Sm*MCM has not been determined, a model generated by sequence alignment to *Hs*MCM suggested a highly hydrophobic lower ligand binding pocket. Consistent with this, we observed higher affinity of cobamides with hydrophobic lower ligands to *Sm*MCM, as well as interference of ring nitrogens with cobamide binding.

On the other hand, sequence alignments suggested that many of the hydrophobic residues predicted to immediately surround the lower ligand are conserved between diverse MCM orthologs that differ in cobamide selectivity. Assuming that the arrangement of the lower ligand binding pocket is similar across MCM orthologs, this suggests that interactions within the lower ligand binding pocket are not sufficient to account for selectivity. In a similar vein, examination of the residues surrounding the lower ligand in the cobamide-bound structures of reductive dehalogenases does not reveal the basis of exclusion of certain cobamides (49). These observations suggest that the lower ligand may have an unknown role in the binding of cobamides to MCM. Consistent with this idea, studies of the kinetics and pH dependence of AdoCbl binding to *P. shermanii* MCM suggest a preassociation step, wherein a cofactor-protein complex is formed prior to displacement of the lower ligand of the cofactor by a histidine residue in the protein (89). The nature of this complex is unknown, but potential interactions between the lower ligand and this conformation of the enzyme could provide an opportunity for lower ligand structure to impact the outcome of binding.

Our analysis of MCM orthologs from *E. coli* and *V. parvula* demonstrates that variations in cobamide selectivity have evolved in organisms with different physiologies. The cobamide selectivity patterns in the three MCM orthologs we examined correlate with the physiologies of the bacteria in two ways. First, in all three cases, each MCM ortholog has highest affinity for the native cobamide produced by the organism, suggesting that cobamide biosynthesis and selectivity of cobamide-dependent enzymes have coevolved. Second, *Sm*MCM is more selective than *Ec*MCM and *Vp*MCM, which is consistent with differences in cobamide biosynthesis, acquisition, and use in these organisms. *S. meliloti* synthesizes cobalamin *de novo* and is incapable of attaching purinyl and phenolyl lower ligands to cobamide precursors (96). Thus, its cobamide-dependent enzymes have likely evolved to function best with cobalamin. In contrast, *E. coli* does not synthesize cobamides *de novo* and instead relies on the importer BtuBFCD to acquire cobamides from the environment (106, 107). Alternatively, *E. coli* can produce a variety of benzimidazolyl and purinyl cobamides when provided with precursors (95), making the ability to use multiple cobamides likely advantageous. Like *S. meliloti*, *V. parvula* synthesizes cobamides *de novo* but can produce both benzimidazolyl and phenolyl cobamides (96, 108) and also encodes membrane transport components adjacent to cobalamin riboswitches (109), which are likely to be cobamide
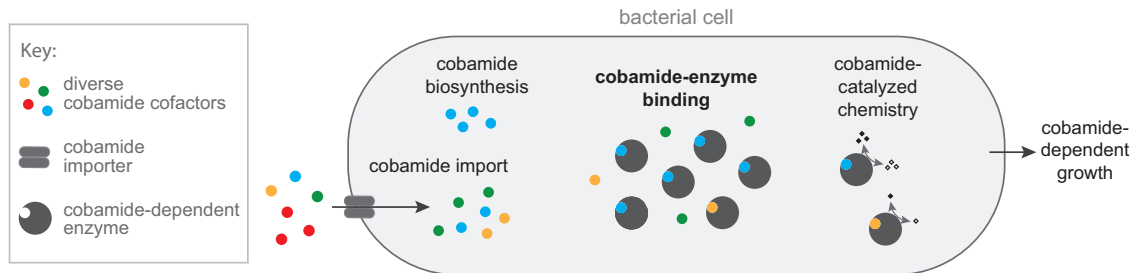
FIG 7 Model describing biochemical determinants of cobamide-dependent growth in bacteria. Cobamides differentially impact bacterial growth due to selective cobamide import and biosynthesis, cobamide-binding selectivity of cobamide-dependent enzymes, and cobamide-dependent catalysis. For MCM-dependent growth of *S. meliloti*, cobamide-binding selectivity is most strongly correlated with cobamide-dependent growth of the organism.

importers (52, 110). Thus, the ability of *Vp*MCM to bind diverse cobamides is similarly consistent with its physiology.

Relative to cobamide binding selectivity, our results suggest that effects of lower ligand structure on the catalytic activity of MCM are minor. Among the cobamides we tested, the maximum differences in *Sm*MCM turnover were 3-fold. We did not observe inhibition of MCM activity with any cobamides, in contrast to the strong inhibition that has been observed with analogs containing variations in the upper ligand or central metal, known as antivitamins (111–113).

In addition to elucidating the biochemical basis of cobamide selectivity in MCM, a major aim of our work was to link biochemical selectivity with cobamide-dependent growth. Our results with benzimidazolyl and purinyl cobamides support the hypothesis that enzyme selectivity is a major determinant of cobamide-dependent growth. Interestingly, although phenolyl cobamides bound *Sm*MCM with high affinity and supported catalysis *in vitro*, high concentrations were required to support growth of *S. meliloti*. This discrepancy can be partially explained by poorer internalization or retention of these cofactors compared to cobalamin (see Fig. S5 in the supplemental material). The observation that the intracellular cobamide concentrations were 50- to 190-fold greater than the amount added to the growth medium (Fig. S5A) suggests that cobamides could be internalized by an uptake mechanism that favors cobalamin, distinct from both BtuBFCD and ECF-CbrT (114, 115), both of which are absent from *S. meliloti*. Thus, we propose a model in which the cobamide-dependent growth of bacteria is influenced not only by binding selectivity of cobamide-dependent enzymes but also by cobamide import (Fig. 7). The lower effectiveness of phenolyl cobamides in supporting growth of *S. meliloti* could additionally be explained by inefficient adenosylation of these cobamides *in vivo*, as MCM requires the adenosyl upper axial ligand for activity. Whether or not adenosyltransferase enzymes, specifically CobA and PduO (116, 117) in *S. meliloti*, are selective with respect to lower ligand structure is unknown.

We and others have proposed the possibility of manipulating microbial communities using cobamides by taking advantage of the differential cobamide-dependent growth of bacteria (39, 118–120). Cobamides are predicted to mediate microbial interactions that are critical to the assembly of complex communities (33, 41, 45, 50, 121–124), so the ability to selectively inhibit or promote the growth of particular species using corrinoids with various lower ligands could be applied to alter the composition of microbial communities in ways that could promote environmental and human health. This possibility hinges on the ability to predict which cobamides support or inhibit growth of an organism of interest, which requires an understanding of the major biochemical determinants of growth. We observed here that the cobamide binding selectivity of a model base-off cobamide-dependent enzyme correlates with growth to a large extent. Thus, uncovering protein residues that confer selectivity would enable prediction of selectivity in cobamide-dependent enzymes, thereby facilitating prediction of the cobamide requirements of organisms of interest. Furthermore, our results suggest that additional steps of cobamide trafficking may be important

determinants of cobamide-dependent growth. Future studies to understand how these various steps depend on cobamide structure will ultimately allow us to better understand, predict, and manipulate microbial interactions.

MATERIALS AND METHODS

Chemical reagents. Chemicals were obtained from the sources indicated: 5′-chloro-5′-deoxyadenosine, Santa Cruz Biotechnology; 7-methylbenzimidazole, Accela; 5-methyl-1H-benzimidazole, Acros Organics; phenol, J. T. Baker; zinc metal, Fisher Scientific; 5-methoxybenzimidazole, purine, and *para*-cresol, Alfa Aesar; methylmalonyl-CoA, methylmalonic acid, coenzyme A, adenosylcobalamin (coenzyme B$_{12}$), cyanocobalamin, dicyanocobinamide, 6-methylpurine, 1H-imidazo[4,5-c]pyridine-4-amine (3-deazaadenine), benzimidazole, adenine hemisulfate, 5-azabenzimidazole, 1H-benzo[d]imidazol-7-amine (7-aminobenzimidazole), 2-methyl-1H-purine-6-amine (2-methyladenine), and bovine serum albumin (BSA), Sigma.

Molecular cloning, protein expression, and purification. *Sm*MCM (locus SM_b20757, *bhbA*) was expressed from the pET28a vector, with an N-terminal hexahistidine (6×His) tag, in *E. coli* BL21(DE3)pLysS (cloning primers are listed in Table S1 in the supplemental material). The expression strain was grown to an optical density at 600 nm (OD$_{600}$) of 0.6 to 0.8 at 37°C, cooled on ice for 15 min, and induced with 1 mM isopropyl-β-D-thiogalactopyranoside (IPTG) for 2.5 h at 37°C. Cells were lysed by sonication in 25 mM Tris-HCl, pH 8.0, 300 mM NaCl, 10 mM imidazole, with 0.5 mM phenylmethylsulfonyl fluoride (PMSF), 1 μg/ml leupeptin, 1 μg/ml pepstatin, and 1 mg/ml lysozyme. Clarified lysate was treated with 0.05% polyethyleneimine. An Äkta Pure 25 fast protein liquid chromatography (FPLC) system was used to purify the protein over a GE 5-ml HisTrap HF column, using a gradient of 21 to 230 mM imidazole in the lysis buffer. Purified protein was dialyzed into 25 mM Tris-HCl, pH 8.0, 300 mM NaCl, 10% glycerol and concentrated with a Vivaspin 10,000-molecular-weight-cutoff (MWCO) protein concentrator. Purity was analyzed by SDS-PAGE (Fig. S7), and protein concentration was determined by A_{280} using the theoretical extinction coefficient 55,810 M^{-1} cm^{-1} (125). *Ec*MCM (locus b2917, *scpA*, previously *sbmA*) was expressed with an N-terminal 6×His tag from a pET28a vector in *E. coli* BL21(DE3), by induction at an OD$_{600}$ of 0.6 to 0.8 with 0.1 mM IPTG, for 3.5 h at 30°C. The protein was purified as described above, and the final concentration was determined by Coomassie blue-stained SDS-PAGE (Fig. S7), using BSA as a standard.

The *V. parvula* genome has two MCM annotations: a heterotetramer (loci Vpar_RS06295 and Vpar_RS06290) and a heterodimer (loci Vpar_RS09005 and Vpar_RS09000). The functionality of both homologs was tested by complementation in *S. meliloti*. The two putative *Vp*MCM enzymes were cloned into the pTH1227 vector and transferred by conjugation into an *S. meliloti bhbA*::Tn5 mutant. Complementation was assessed by growth in M9 liquid medium containing L-isoleucine and L-valine (see "*S. meliloti* growth assays" below for additional details). *S. meliloti* coexpressing Vpar_RS09005 and Vpar_RS09000 showed identical growth to a strain expressing *Sm*MCM from pTH1227 and was selected for *in vitro* studies.

The α subunit of *Vp*MCM (encoded by Vpar_RS09005) was expressed with an N-terminal 6×His tag from the pET-Duet expression vector in *E. coli* BL21(DE3). Protein expression was induced with 520 μM IPTG for 6 h at 30°C. The protein was batch purified by nickel affinity and subsequently purified by FPLC using a HiTrapQ column with an NaCl gradient from 50 to 500 mM in 20 Tris-HCl, pH 8.0, 10% glycerol. The β subunit of *Vp*MCM (encoded by Vpar_RS09000) was expressed separately with an N-terminal 6×His tag from the pET-Duet expression vector in *E. coli* BL21(DE3). Expression was induced with 1 mM IPTG for 22 h at 16°C, and the protein was purified using nickel-affinity chromatography as described for *Sm*MCM. Purified protein was dialyzed into 25 mM Tris-HCl, pH 8.0, 300 mM NaCl, 10% glycerol, and 1 mM β-mercaptoethanol. Concentration of pure α and β subunits (Fig. S7) was determined by absorbance at 280 nm (A_{280}) using the theoretically calculated extinction coefficients 75,290 M^{-1} cm^{-1} and 74,260 M^{-1} cm^{-1}, respectively (125). Equimolar amounts of α and β subunits were combined during the setup of fluorescence binding assays.

E. coli thiokinase containing an N-terminal 6×His tag was expressed from a vector provided by Gregory Campanello from the laboratory of Ruma Banerjee. Expression was induced with 1 mM IPTG in *E. coli* BL21(DE3)pLysS at 28°C for 3 h. The protein was purified as a heterodimer using nickel-affinity chromatography as described above. His-tagged *Rhodopseudomonas palustris* MatB (126) was expressed from a pET16b expression plasmid provided by Omer Ad from the laboratory of Michelle Chang. The protein was overexpressed in *E. coli* BL21(DE3) at 16°C overnight, after induction with 1 mM IPTG, and purified by nickel-affinity chromatography as indicated above. Thiokinase and MatB concentrations were determined by Coomassie blue-stained SDS-PAGE, using BSA as a standard.

Guided biosynthesis, extraction, and purification of cobamides. *Sporomusa ovata* strain DSM 2662 was used for the production of its native cobamide, [Cre]Cba, and for production of [Phe]Cba, [5-MeBza]Cba, [Bza]Cba, [5-OHBza]Cba, [7-MeBza]Cba, and [7-AmBza]Cba, by guided biosynthesis as previously described (44). 5-OHBza was synthesized as described previously (96). *Salmonella enterica* serovar Typhimurium strain LT2 and *Propionibacterium acidipropionici* strain DSM 20273 were used for production of [Ade]Cba (47, 127). [2-MeAde]Cba, [Pur]Cba, [6-AzaBza]Cba, [3-DeazaAde]Cba, and [6-MePur]Cba were produced by guided biosynthesis in *P. acidipropionici*. Cobamides were extracted as previously described (47) and purified by high-performance liquid chromatography (HPLC) using previously published methods (47, 96, 128) as well as additional methods listed in Table S2. In many cases, more than one method was required to achieve high purity. Identity of cobamides was confirmed by liquid chromatography (LC) coupled to mass spectrometry (MS) using an Agilent 1260 LC/6120 quadrupole MS instrument. The orientation of the lower ligands of [7-MeBza]Cba, [7-AmBza]Cba, [3-

DeazaAde]Cba, and [6-MePur]Cba is likely to be analogous to the lower ligand orientation in purinyl cobamides (127, 129). This assumption is supported by the absorbance spectra of these cobamides under acidic conditions, which reveal a base-on conformation (Fig. S8); the opposite orientation of the amino and methyl substituents would create steric interference between the lower ligand and corrin ring, which would be expected to weaken the coordination bond and favor a base-off conformation, especially at low pH. The orientation of the lower ligands in [Pur]Cba and [6-AzaBza]Cba was not determined.

Chemical adenosylation of cobamides. Cobamide adenosylation was performed as previously described (128, 130). Briefly, cobamides at concentrations of 0.5 to 1 mM were reduced with activated zinc metal under anaerobic conditions, with vigorous stirring for 0.5 to 2 h. 5′-Chloro-5′-deoxyadenosine was added, and adenosylation was allowed to proceed for 1 to 3 h in the dark. The progress of the reaction was monitored by HPLC. Following adenosylation, cobamides were desalted using a C_{18} SepPak (Waters), purified by HPLC, desalted again, dried, and stored at −20°C or −80°C.

Cobamide quantification. Purified cobamides were dissolved in water and quantified by UV-Vis spectrophotometry on a BioTek Synergy 2 plate reader using the following extinction coefficients: for cyanylated benzimidazolyl cobamides, $\varepsilon_{518} = 7.4 \times 10^3$ M^{-1} cm^{-1} (131); for cyanylated purinyl cobamides, $\varepsilon_{548} = 7.94 \times 10^3$ M^{-1} cm^{-1} (132); for cyanylated phenolyl cobamides, $\varepsilon_{495} = 9.523 \times 10^3$ M^{-1} cm^{-1} (133); for adenosylated benzimidazolyl cobamides (AdoCbl, Ado[5-MeBza]Cba, Ado[Bza]Cba, Ado[5-OHBza]Cba, Ado[7-MeBza]Cba, and Ado[7-AmBza]Cba), which are predominantly base-on in water, $\varepsilon_{522} = 8.0$ mM^{-1} cm^{-1} (131); for adenosylated purinyl cobamides (Ado[Ade]Cba, Ado[2-MeAde]Cba, and Ado[Pur]Cba), which are predominantly base-off in water, and phenolyl cobamides (Ado[Cre]Cba and Ado[Phe]Cba), which are base-off, $\varepsilon_{458} = 8.8$ mM^{-1} cm^{-1} (132); for adenosylated azabenzimidazolyl cobamides (Ado[3-DeazaAde]Cba, Ado[6-AzaBza]Cba, and Ado[6-MePur]Cba), which are a mixture of base-on and base-off in water, the concentration was estimated from the average of concentrations calculated using the extinction coefficients above.

Fluorescence binding assays. An in vitro assay previously described for measuring binding of AdoCbl to P. shermanii MCM (89) was adapted to a 96-well format: MCM (0.2 µM) was combined with a range of cobamide concentrations (as specified in each experiment) in a black 96-well plate in 50 mM potassium phosphate, pH 7.5, with 1 mM dithiothreitol (DTT), on ice. All steps involving cobamides were conducted in the dark. The plate was centrifuged for 1 min at 3,800 rpm to level the surface of the liquid in each well. The plate was then incubated for 40 min at 30°C to allow binding, with a brief shaking step after 30 min. Preliminary experiments showed that this time is sufficient for equilibration. Following incubation, fluorescence emission at 340 nm (5-nm slit width) was measured upon excitation at 282 nm (5-nm slit width) using a Tecan Infinite M1000 Pro plate reader. Fluorescence, normalized to the initial value, was plotted as a function of cobamide concentration, and fitted to the following equation (134):

$$\frac{F}{F_0} = 1 + \frac{\Delta F_{\max}}{F_0} \frac{([E] + [L] + K_d) - \sqrt{([E] + [L] + K_d)^2 - 4[E][L]}}{2[E]}$$

where F is fluorescence, F_0 is initial fluorescence, $[E]$ is total enzyme concentration, $[L]$ is total ligand concentration, and K_d is the binding dissociation constant.

Filtration binding assay. Cobamides (10 µM) with and without MCM (15 µM) were incubated in 100 mM Tris, 50 mM phosphate, pH 7.5, at 30°C for 40 min, transferred to Nanosep 10K Omega centrifugal devices (Pall Corporation), and centrifuged for 5 min at 13,900 × g to separate unbound cobamides from enzyme-bound cobamides. The UV-Vis spectra of the filtrates were recorded on a BioTek Synergy 2 plate reader.

Structural modeling. A model of SmMCM was generated using the Swiss-Model software (135) based on the known crystal structure of Homo sapiens MCM (HsMCM) (PDB ID 2XIJ) (97). No major differences were observed in the B_{12}-binding domain between SmMCM models generated from HsMCM and Propionibacterium freudenreichii MCM (PDB ID 4REQ) (61).

Maestro (136) was used to generate a model of HsMCM bound to [Ade]Cba. The initial structure of HsMCM bound to cobalamin (PDB ID 2XIQ) (97) was prepared using standard methods. A constrained energy minimization (atoms within 10 Å of cobalamin freely moving; atoms within a second 10-Å shell constrained by a force constant of 200; remaining structure frozen) was performed using MacroModel (137). The structure of the lower ligand was then modified to adenine, and the constrained energy minimization was repeated to generate a model of the lower ligand binding pocket bound to [Ade]Cba.

Enzymatic synthesis of (R)-methylmalonyl-CoA. (R)-Methylmalonyl-CoA synthesis reaction mixtures contained the following in 10 ml: 100 mM sodium phosphate (pH 7.5), 20 mM MgCl$_2$, 5 mM ATP, 10 mM methylmalonic acid, 2 mM coenzyme A, 5 mM β-mercaptoethanol, and 1.5 µM purified MatB protein. After combining ingredients on ice, the reaction mixture was incubated at 37°C for 1 h. The reaction mixture was then frozen in liquid nitrogen and lyophilized. To purify (R)-methylmalonyl-CoA, the dried reaction mixture was resuspended in 3.2 ml water, the protein was precipitated with 200 µl trichloroacetic acid, precipitate was pelleted, supernatant was neutralized with 200 µl of 10 M NaOH, and salts and remaining starting materials were removed using a C_{18} SepPak column (Waters) (loaded in 0.1% formic acid and washed with water, methylmalonyl-CoA was eluted with 50% methanol in water). Formation of (R)-methylmalonyl-CoA was initially verified by ^{1}H nuclear magnetic resonance (NMR) and in subsequent preparations by HPLC (Table S2). The concentration of (R)-methylmalonyl-CoA was determined using an extinction coefficient of 12.2 mM^{-1} cm^{-1} at 259 nm.

MCM activity assays. A thiokinase-coupled, spectrophotometric MCM activity assay was adapted from previous work (138), except that ADP was used instead of GDP, and the experiment was conducted in 96-well plates. Final concentrations of reagents in the assays were as follows: Tris-phosphate buffer (pH

7.5), 100 mM Tris, 50 mM phosphate; dithionitrobenzoate (DTNB), 400 μM; ADP, 1 mM; MgCl$_2$, 10 mM; (R)-methylmalonyl-CoA, 0 to 4 mM; thiokinase, 5 μM; MCM, 50 nM; and cobamides, 2 μM. Preliminary experiments were conducted to ensure that concentrations of thiokinase, DTNB, and cobamides were not rate limiting.

Three separate mixes were prepared, all in 1$\times$ Tris-phosphate buffer: an assay mix containing DTNB, ADP, and MgCl$_2$; a substrate mix containing (R)-methylmalonyl-CoA; and an enzyme mix containing thiokinase, MCM, and cobamides. All steps involving cobamides were conducted in the dark. The assay and enzyme mixes were prepared as a master mix and aliquoted into 96-well plates; substrate mixes were prepared in individual wells, in triplicate. All components were incubated at 30°C for 40 min to equilibrate temperature and allow prebinding of cobamides and MCM. After incubation, one replicate at a time, the substrate mix was added to the assay mix, followed by the enzyme mix. Absorbance at 412 nm (A_{412}) was recorded immediately after addition of enzyme and for 1 to 3 min, every 3 s, on a BioTek Synergy 2 plate reader. The increase in A_{412} in reaction mixtures lacking substrate was subtracted from all readings, to account for reactivity of DTNB with thiols on protein surfaces. A_{412} values were converted to concentration of free CoA using a path-length correction determined for the reaction volume and extinction coefficient of 14,150 M^{-1} cm^{-1}.

S. meliloti growth assays. MCM-dependent growth experiments were performed with S. meliloti strain Rm1021 cobD::gus Gm^r metH::Tn5 ΔnrdJ pMS03-nrdAB$_{Ec}$$^+$, which lacks cobamide-dependent enzymes other than MCM and does not synthesize cobalamin. cobD is required for cobalamin biosynthesis (139), metH encodes methionine synthase (139–141), and nrdJ encodes ribonucleotide reductase (142). Because nrdJ is essential, the E. coli cobamide-independent ribonucleotide reductase encoded by nrdA and nrdB was expressed from the pMS03 plasmid (143). The strain was precultured in M9 medium (144) (modified concentration of MgSO$_4$: 1 mM) containing 0.1% sucrose, 2 g/liter isoleucine, 2 g/liter valine, 1 g/liter methionine, and 20 μg/ml gentamicin, with shaking at 30°C. After 2 days, cells were washed and diluted to an OD$_{600}$ of 0.02 into M9 medium containing 4 g/liter isoleucine, 4 g/liter valine, 1 g/liter methionine, 20 μg/ml gentamicin, and cobamides at various concentrations as indicated for each experiment, in 384-well plates. The plates were incubated at 30°C for 145 h in a BioTek Synergy 2 plate reader with linear shaking at 1,140 cpm. OD$_{600}$ was measured in 1-h increments.

For quantification of intracellular cobamides in S. meliloti, the strain above was precultured as described above, diluted into 50 ml of M9 medium containing 0.2% sucrose and various cobamides, and grown for 48 h (until OD$_{600}$ reached 0.6 to 0.8). Cobamides were extracted from cell pellets as previously described (47), using 5 ml of methanol containing 500 μg of potassium cyanide. A partial purification by means of a wash step with 20% methanol in water was included during the SepPak desalting procedure. Extracted cobamides were quantified by HPLC using peak areas at 525 nm and external standard curves, and cellular cobamide concentrations were calculated assuming 8 $\times$ 10^8 cells/ml at an OD$_{600}$ of 1.0 and a cellular volume of 1 μm^3.

SUPPLEMENTAL MATERIAL

Supplemental material for this article may be found at https://doi.org/10.1128/mBio .01303-19.

FIG S1, EPS file, 2.3 MB.
FIG S2, EPS file, 1.7 MB.
FIG S3, EPS file, 1 MB.
FIG S4, TIF file, 2.2 MB.
FIG S5, EPS file, 1.9 MB.
FIG S6, TIF file, 2 MB.
FIG S7, TIF file, 2 MB.
FIG S8, EPS file, 2.9 MB.
TABLE S1, DOCX file, 0.01 MB.
TABLE S2, DOCX file, 0.01 MB.

REFERENCES

1. Brodie JD, Burke GT, Mangum JH. 1970. Methylcobalamin as an intermediate in mammalian methionine biosynthesis. Biochemistry 9:4297–4302. https://doi.org/10.1021/bi00824a009.

2. Fenton WA, Hack AM, Willard HF, Gertler A, Rosenberg LE. 1982. Purification and properties of methylmalonyl coenzyme A mutase from human liver. Arch Biochem Biophys 214:815–823. https://doi.org/10.1016/0003-9861(82)90088-1.

3. Licht S, Gerfen GJ, Stubbe J. 1996. Thiyl radicals in ribonucleotide reductases. Science 271:477–481. https://doi.org/10.1126/science.271.5248.477.

4. Berg IA, Kockelkorn D, Buckel W, Fuchs G. 2007. A 3-hydroxypropionate/4-hydroxybutyrate autotrophic carbon dioxide assimilation pathway in Archaea. Science 318:1782–1786. https://doi.org/10.1126/science.1149976.

5. Ljungdahl LG. 1986. The autotrophic pathway of acetate synthesis in acetogenic bacteria. Annu Rev Microbiol 40:415–450. https://doi.org/10.1146/annurev.mi.40.100186.002215.

6. Krasotkina J, Walters T, Maruya KA, Ragsdale SW. 2001. Characterization of the B_{12}- and iron-sulfur-containing reductive dehalogenase from Desulfitobacterium chlororespirans. J Biol Chem 276:40991–40997. https://doi.org/10.1074/jbc.M106217200.

7. Scarlett FA, Turner JM. 1976. Microbial metabolism of amino alcohols. Ethanolamine catabolism mediated by coenzyme B_{12}-dependent ethanolamine ammonia-lyase in Escherichia coli and Klebsiella aerogenes. J Gen Microbiol 95:173–176. https://doi.org/10.1099/00221287-95-1-173.

8. Stupperich E, Konle R. 1993. Corrinoid-dependent methyl transfer reactions are involved in methanol and 3,4-dimethoxybenzoate metabolism by Sporomusa ovata. Appl Environ Microbiol 59:3110–3116.

9. Jeter RM. 1990. Cobalamin-dependent 1,2-propanediol utilization by Salmonella typhimurium. J Gen Microbiol 136:887–896. https://doi.org/10.1099/00221287-136-5-887.

10. Forage RG, Foster MA. 1982. Glycerol fermentation in Klebsiella pneumoniae: functions of the coenzyme B_{12}-dependent glycerol and diol dehydratases. J Bacteriol 149:413–419.

11. Erb TJ, Retey J, Fuchs G, Alber BE. 2008. Ethylmalonyl-CoA mutase from Rhodobacter sphaeroides defines a new subclade of coenzyme B_{12}-dependent acyl-CoA mutases. J Biol Chem 283:32283–32293. https://doi.org/10.1074/jbc.M805527200.

12. Vrijbloed JW, Zerbe-Burkhardt K, Ratnatilleke A, Grubelnik-Leiser A, Robinson JA. 1999. Insertional inactivation of methylmalonyl coenzyme A (CoA) mutase and isobutyryl-CoA mutase genes in Streptomyces cinnamonensis: influence on polyketide antibiotic biosynthesis. J Bacteriol 181:5600–5605.

13. Korotkova N, Chistoserdova L, Kuksa V, Lidstrom ME. 2002. Glyoxylate regeneration pathway in the methylotroph Methylobacterium extorquens AM1. J Bacteriol 184:1750–1758. https://doi.org/10.1128/jb.184.6.1750-1758.2002.

14. Ferguson DJ, Jr, Krzycki JA. 1997. Reconstitution of trimethylamine-dependent coenzyme M methylation with the trimethylamine corrinoid protein and the isozymes of methyltransferase II from Methanosarcina barkeri. J Bacteriol 179:846–852. https://doi.org/10.1128/jb.179.3.846-852.1997.

15. Barker HA. 1985. Beta-methylaspartate-glutamate mutase from Clostridium tetanomorphum. Methods Enzymol 113:121–133. https://doi.org/10.1016/s0076-6879(85)13026-0.

16. Chang CH, Frey PA. 2000. Cloning, sequencing, heterologous expression, purification, and characterization of adenosylcobalamin-dependent D-lysine 5,6-aminomutase from Clostridium sticklandii. J Biol Chem 275:106–114. https://doi.org/10.1074/jbc.275.1.106.

17. Chen HP, Wu SH, Lin YL, Chen CM, Tsay SS. 2001. Cloning, sequencing, heterologous expression, purification, and characterization of adenosylcobalamin-dependent D-ornithine aminomutase from Clostridium sticklandii. J Biol Chem 276:44744–44750. https://doi.org/10.1074/jbc.M108365200.

18. Allen KD, Wang SC. 2014. Initial characterization of Fom3 from Streptomyces wedmorensis: the methyltransferase in fosfomycin biosyn-

thesis. Arch Biochem Biophys 543:67–73. https://doi.org/10.1016/j.abb.2013.12.004.

19. Blaszczyk AJ, Silakov A, Zhang B, Maiocco SJ, Lanz ND, Kelly WL, Elliott SJ, Krebs C, Booker SJ. 2016. Spectroscopic and electrochemical characterization of the iron-sulfur and cobalamin cofactors of TsrM, an unusual radical S-adenosylmethionine methylase. J Am Chem Soc 138:3416–3426. https://doi.org/10.1021/jacs.5b12592.

20. Bridwell-Rabb J, Zhong A, Sun HG, Drennan CL, Liu HW. 2017. A B_{12}-dependent radical SAM enzyme involved in oxetanocin A biosynthesis. Nature 544:322–326. https://doi.org/10.1038/nature21689.

21. Kim HJ, Liu YN, McCarty RM, Liu HW. 2017. Reaction catalyzed by GenK, a cobalamin-dependent radical S-adenosyl-L-methionine methyltransferase in the biosynthetic pathway of gentamicin, proceeds with retention of configuration. J Am Chem Soc 139:16084–16087. https://doi.org/10.1021/jacs.7b09890.

22. Pierre S, Guillot A, Benjdia A, Sandstrom C, Langella P, Berteau O. 2012. Thiostrepton tryptophan methyltransferase expands the chemistry of radical SAM enzymes. Nat Chem Biol 8:957–959. https://doi.org/10.1038/nchembio.1091.

23. Werner WJ, Allen KD, Hu K, Helms GL, Chen BS, Wang SC. 2011. In vitro phosphinate methylation by PhpK from Kitasatospora phosalacinea. Biochemistry 50:8986–8988. https://doi.org/10.1021/bi201220r.

24. Marous DR, Lloyd EP, Buller AR, Moshos KA, Grove TL, Blaszczyk AJ, Booker SJ, Townsend CA. 2015. Consecutive radical S-adenosylmethionine methylations form the ethyl side chain in thienamycin biosynthesis. Proc Natl Acad Sci U S A 112:10354–10358. https://doi.org/10.1073/pnas.1508615112.

25. Jung WS, Kim E, Yoo YJ, Ban YH, Kim EJ, Yoon YJ. 2014. Characterization and engineering of the ethylmalonyl-CoA pathway towards the improved heterologous production of polyketides in Streptomyces venezuelae. Appl Microbiol Biotechnol 98:3701–3713. https://doi.org/10.1007/s00253-013-5503-8.

26. Ortiz-Guerrero JM, Polanco MC, Murillo FJ, Padmanabhan S, Elías-Arnanz M. 2011. Light-dependent gene regulation by a coenzyme B_{12}-based photoreceptor. Proc Natl Acad Sci U S A 108:7565–7570. https://doi.org/10.1073/pnas.1018972108.

27. Gough SP, Petersen BO, Duus JO. 2000. Anaerobic chlorophyll isocyclic ring formation in Rhodobacter capsulatus requires a cobalamin cofactor. Proc Natl Acad Sci U S A 97:6908–6913. https://doi.org/10.1073/pnas.97.12.6908.

28. Parks JM, Johs A, Podar M, Bridou R, Hurt RA, Jr, Smith SD, Tomanicek SJ, Qian Y, Brown SD, Brandt CC, Palumbo AV, Smith JC, Wall JD, Elias DA, Liang L. 2013. The genetic basis for bacterial mercury methylation. Science 339:1332–1335. https://doi.org/10.1126/science.1230667.

29. Miles ZD, McCarty RM, Molnar G, Bandarian V. 2011. Discovery of epoxyqueuosine (oQ) reductase reveals parallels between halorespiration and tRNA modification. Proc Natl Acad Sci U S A 108:7368–7372. https://doi.org/10.1073/pnas.1018636108.

30. Yaneva N, Schuster J, Schäfer F, Lede V, Przybylski D, Paproth T, Harms H, Müller RH, Rohwerder T. 2012. Bacterial acyl-CoA mutase specifically catalyzes coenzyme B_{12}-dependent isomerization of 2-hydroxyisobutyryl-CoA and (S)-3-hydroxybutyryl-CoA. J Biol Chem 287:15502–15511. https://doi.org/10.1074/jbc.M111.314690.

31. Cracan V, Banerjee R. 2012. Novel coenzyme B_{12}-dependent interconversion of isovaleryl-CoA and pivalyl-CoA. J Biol Chem 287:3723–3732. https://doi.org/10.1074/jbc.M111.320051.

32. Romine MF, Rodionov DA, Maezato Y, Anderson LN, Nandhikonda P, Rodionova IA, Carre A, Li X, Xu C, Clauss TR, Kim YM, Metz TO, Wright AT. 2017. Elucidation of roles for vitamin B_{12} in regulation of folate, ubiquinone, and methionine metabolism. Proc Natl Acad Sci U S A 114:e1205–e1214. https://doi.org/10.1073/pnas.1612360114.

33. Shelton AN, Seth EC, Mok KC, Han AW, Jackson SN, Haft DR, Taga ME. 2019. Uneven distribution of cobamide biosynthesis and dependence in bacteria predicted by comparative genomics. ISME J 13:789–804. https://doi.org/10.1038/s41396-018-0304-9.

34. Banerjee R, Ragsdale SW. 2003. The many faces of vitamin B_{12}: catalysis

by cobalamin-dependent enzymes. Annu Rev Biochem 72:209–247. https://doi.org/10.1146/annurev.biochem.72.121801.161828.

35. Bridwell-Rabb J, Drennan CL. 2017. Vitamin B_{12} in the spotlight again. Curr Opin Chem Biol 37:63–70. https://doi.org/10.1016/j.cbpa.2017.01.013.

36. Hodgkin DC, Kamper J, Mackay M, Pickworth J, Trueblood KN, White JG. 1956. Structure of vitamin B_{12}. Nature 178:64–66. https://doi.org/10.1038/178064a0.

37. Kräutler B, Fieber W, Ostermann S, Fasching M, Ongania K-H, Gruber K, Kratky C, Mikl C, Siebert A, Diekert G. 2003. The cofactor of tetrachloroethene reductive dehalogenase of *Dehalospirillum multivorans* is norpseudo-B_{12}, a new type of a natural corrinoid. Helvetica 86:3698–3716. https://doi.org/10.1002/hlca.200390313.

38. Keller S, Treder A, von Reuss SH, Escalante-Semerena JC, Schubert T. 2016. The SMUL_1544 gene product governs norcobamide biosynthesis in the tetrachloroethene-respiring bacterium *Sulfurospirillum multivorans*. J Bacteriol 198:2236–2243. https://doi.org/10.1128/JB.00289-16.

39. Yan J, Bi M, Bourdon AK, Farmer AT, Wang P-H, Molenda O, Quaile AT, Jiang N, Yang Y, Yin Y, Şimşir B, Campagna SR, Edwards EA, Löffler FE. 2018. Purinyl-cobamide is a native prosthetic group of reductive dehalogenases. Nat Chem Biol 14:8–14. https://doi.org/10.1038/nchembio.2512.

40. Allen RH, Stabler SP. 2008. Identification and quantitation of cobalamin and cobalamin analogues in human feces. Am J Clin Nutr 87:1324–1335. https://doi.org/10.1093/ajcn/87.5.1324.

41. Men Y, Seth EC, Yi S, Crofts TS, Allen RH, Taga ME, Alvarez-Cohen L. 2015. Identification of specific corrinoids reveals corrinoid modification in dechlorinating microbial communities. Environ Microbiol 17:4873–4884. https://doi.org/10.1111/1462-2920.12500.

42. Girard CL, Santschi DE, Stabler SP, Allen RH. 2009. Apparent ruminal synthesis and intestinal disappearance of vitamin B_{12} and its analogs in dairy cows. J Dairy Sci 92:4524. https://doi.org/10.3168/jds.2009-2049.

43. Renz P 1999. Biosynthesis of the 5,6-dimethylbenzimidazole moiety of cobalamin and of the other bases found in natural corrinoids, p 557–566. *In* Banerjee R (ed), Chemistry and biochemistry of B_{12}. John Wiley & Sons, Inc, New York, NY.

44. Mok KC, Taga ME. 2013. Growth inhibition of *Sporomusa ovata* by incorporation of benzimidazole bases into cobamides. J Bacteriol 195:1902–1911. https://doi.org/10.1128/JB.01282-12.

45. Helliwell KE, Lawrence AD, Holzer A, Kudahl UJ, Sasso S, Krautler B, Scanlan DJ, Warren MJ, Smith AG. 2016. Cyanobacteria and eukaryotic algae use different chemical variants of vitamin B_{12}. Curr Biol 26:999–1008. https://doi.org/10.1016/j.cub.2016.02.041.

46. Watanabe F, Nakano Y, Stupperich E. 1992. Different corrinoid specificities for cell growth and cobalamin uptake in *Euglena gracilis* Z. J Gen Microbiol 138:1807–1813. https://doi.org/10.1099/00221287-138-9-1807.

47. Yi S, Seth EC, Men YJ, Stabler SP, Allen RH, Alvarez-Cohen L, Taga ME. 2012. Versatility in corrinoid salvaging and remodeling pathways supports corrinoid-dependent metabolism in *Dehalococcoides mccartyi*. Appl Environ Microbiol 78:7745–7752. https://doi.org/10.1128/AEM.02150-12.

48. Yan J, Şimşir B, Farmer AT, Bi M, Yang Y, Campagna SR, Löffler FE. 2016. The corrinoid cofactor of reductive dehalogenases affects dechlorination rates and extents in organohalide-respiring *Dehalococcoides mccartyi*. ISME J 10:1092–1101. https://doi.org/10.1038/ismej.2015.197.

49. Keller S, Kunze C, Bommer M, Paetz C, Menezes RC, Svatoš A, Dobbek H, Schubert T. 2018. Selective utilization of benzimidazolylnorcobamides as cofactors by the tetrachloroethene reductive dehalogenase of *Sulfurospirillum multivorans*. J Bacteriol 200:e00584-17. https://doi.org/10.1128/JB.00584-17.

50. Degnan PH, Barry NA, Mok KC, Taga ME, Goodman AL. 2014. Human gut microbes use multiple transporters to distinguish vitamin B_{12} analogs and compete in the gut. Cell Host Microbe 15:47–57. https://doi.org/10.1016/j.chom.2013.12.007.

51. Zhang Y, Rodionov DA, Gelfand MS, Gladyshev VN. 2009. Comparative genomic analyses of nickel, cobalt and vitamin B_{12} utilization. BMC Genomics 10:78. https://doi.org/10.1186/1471-2164-10-78.

52. Rodionov DA, Vitreschak AG, Mironov AA, Gelfand MS. 2003. Comparative genomics of the vitamin B_{12} metabolism and regulation in prokaryotes. J Biol Chem 278:41148–41159. https://doi.org/10.1074/jbc.M305837200.

53. Yamanishi M, Yunoki M, Tobimatsu T, Sato H, Matsui J, Dokiya A, Iuchi Y, Oe K, Suto K, Shibata N, Morimoto Y, Yasuoka N, Toraya T. 2002. The crystal structure of coenzyme B_{12}-dependent glycerol dehydratase in complex with cobalamin and propane-1,2-diol. Eur J Biochem 269:4484–4494. https://doi.org/10.1046/j.1432-1033.2002.03151.x.

54. Larsson KM, Logan DT, Nordlund P 2010. Structural basis for adenosylcobalamin activation in AdoCbl-dependent ribonucleotide reductases. ACS Chem Biol 5:933–942. https://doi.org/10.1021/cb1000845.

55. Shibata N, Sueyoshi Y, Higuchi Y, Toraya T. 2018. Direct participation of a peripheral side chain of a corrin ring in coenzyme B_{12} catalysis. Angew Chem Int Ed Engl 57:7830–7835. https://doi.org/10.1002/anie.201803591.

56. Conrad KS, Jordan CD, Brown KL, Brunold TC. 2015. Spectroscopic and computational studies of cobalamin species with variable lower axial ligation: implications for the mechanism of Co-C bond activation by class I cobalamin-dependent isomerases. Inorg Chem 54:3736–3747. https://doi.org/10.1021/ic502665x.

57. Brown KL. 2006. The enzymatic activation of coenzyme B_{12}. Dalton Trans (9):1123–1133. https://doi.org/10.1039/b517599m.

58. Kozlowski PM, Zgierski MZ. 2004. Electronic and steric influence of trans axial base on the stereoelectronic properties of cobalamins. J Phys Chem B 108:14163–14170. https://doi.org/10.1021/jp040373c.

59. Poppe L, Bothe H, Bröker G, Buckel W, Stupperich E, Rétey J. 2000. Elucidation of the coenzyme binding mode of further B_{12}-dependent enzymes using a base-off analogue of coenzyme B_{12}. J Mol Catal B Enzym 10:345–350. https://doi.org/10.1016/S1381-1177(00)00136-3.

60. Poppe L, Stupperich E, Hull WE, Buckel T, Retey J. 1997. A base-off analogue of coenzyme-B_{12} with a modified nucleotide loop; ^{1}H-NMR structure analysis and kinetic studies with (*R*)-methylmalonyl-CoA mutase, glycerol dehydratase, and diol dehydratase. Eur J Biochem 250:303–307. https://doi.org/10.1111/j.1432-1033.1997.0303a.x.

61. Mancia F, Keep NH, Nakagawa A, Leadlay PF, McSweeney S, Rasmussen B, Bosecke P, Diat O, Evans PR. 1996. How coenzyme B_{12} radicals are generated: the crystal structure of methylmalonyl-coenzyme A mutase at 2 Å resolution. Structure 4:339–350. https://doi.org/10.1016/S0969-2126(96)00037-8.

62. Bommer M, Kunze C, Fesseler J, Schubert T, Diekert G, Dobbek H. 2014. Structural basis for organohalide respiration. Science 346:455–458. https://doi.org/10.1126/science.1258118.

63. Drennan C, Huang S, Drummond J, Matthews R, Lidwig M. 1994. How a protein binds B_{12}: a 3.0 Å X-ray structure of B_{12}-binding domains of methionine synthase. Science 266:1669–1674. https://doi.org/10.1126/science.7992050.

64. Gruber K, Reitzer R, Kratky C. 2001. Radical shuttling in a protein: ribose pseudorotation controls alkyl-radical transfer in the coenzyme B_{12} dependent enzyme glutamate mutase. Angew Chem Int Ed 40:3377–3380. https://doi.org/10.1002/1521-3773(20010917)40:18<3377::AID-ANIE3377>3.0.CO;2-8.

65. Berkovitch F, Behshad E, Tang KH, Enns EA, Frey PA, Drennan CL. 2004. A locking mechanism preventing radical damage in the absence of substrate, as revealed by the x-ray structure of lysine 5,6-aminomutase. Proc Natl Acad Sci U S A 101:15870–15875. https://doi.org/10.1073/pnas.0407074101.

66. Wolthers KR, Levy C, Scrutton NS, Leys D. 2010. Large-scale domain dynamics and adenosylcobalamin reorientation orchestrate radical catalysis in ornithine 4,5-aminomutase. J Biol Chem 285:13942–13950. https://doi.org/10.1074/jbc.M109.068908.

67. Jost M, Cracan V, Hubbard PA, Banerjee R, Drennan CL. 2015. Visualization of a radical B_{12} enzyme with its G-protein chaperone. Proc Natl Acad Sci U S A 112:2419–2424. https://doi.org/10.1073/pnas.1419582112.

68. Payne KA, Fisher K, Sjuts H, Dunstan MS, Bellina B, Johannissen L, Barran P, Hay S, Rigby SE, Leys D. 2015. Epoxyqueuosine reductase structure suggests a mechanism for cobalamin-dependent tRNA modification. J Biol Chem 290:27572–27581. https://doi.org/10.1074/jbc.M115.685693.

69. Payne KA, Quezada CP, Fisher K, Dunstan MS, Collins FA, Sjuts H, Levy C, Hay S, Rigby SE, Leys D. 2015. Reductive dehalogenase structure suggests a mechanism for B_{12}-dependent dehalogenation. Nature 517:513–516. https://doi.org/10.1038/nature13901.

70. Kurteva-Yaneva N, Zahn M, Weichler M-T, Starke R, Harms H, Müller RH, Sträter N, Rohwerder T. 2015. Structural basis of the stereospecificity of bacterial B_{12}-dependent 2-hydroxyisobutyryl-CoA mutase. J Biol Chem 290:9727–9737. https://doi.org/10.1074/jbc.M115.645689.

71. Tanioka Y, Miyamoto E, Yabuta Y, Ohnishi K, Fujita T, Yamaji R, Misono H, Shigeoka S, Nakano Y, Inui H, Watanabe F. 2010. Methyladeninylcobamide functions as the cofactor of methionine synthase in a cyano-

bacterium, *Spirulina platensis* NIES-39. FEBS Lett 584:3223–3226. https://doi.org/10.1016/j.febslet.2010.06.013.

72. Lengyel P, Mazumder R, Ochoa S. 1960. Mammalian methylmalonyl isomerase and vitamin B_{12} coenzymes. Proc Natl Acad Sci U S A 46:1312–1318. https://doi.org/10.1073/pnas.46.10.1312.

73. Barker HA, Smyth RD, Weissbach H, Toohey JI, Ladd JN, Volcani BE. 1960. Isolation and properties of crystalline cobamide coenzymes containing benzimidazole or 5,6-dimethylbenzimidazole. J Biol Chem 235:480–488.

74. Dowling DP, Croft AK, Drennan CL. 2012. Radical use of Rossmann and TIM barrel architectures for controlling coenzyme B_{12} chemistry. Annu Rev Biophys 41:403–427. https://doi.org/10.1146/annurev-biophys-050511-102225.

75. Hosotani K, Yokota A, Nakano Y, Kitaoka S. 1980. The metabolic pathway of propionate in *Euglena gracilis* z grown under illumination. Agric Biol Chem 44:1097–1103. https://doi.org/10.1271/bbb1961.44.1097.

76. Savvi S, Warner DF, Kana BD, McKinney JD, Mizrahi V, Dawes SS. 2008. Functional characterization of a vitamin B_{12}-dependent methylmalonyl pathway in *Mycobacterium tuberculosis*: implications for propionate metabolism during growth on fatty acids. J Bacteriol 190:3886. https://doi.org/10.1128/JB.01767-07.

77. Fenton WA, Gravel RA, Rosenblatt DS. 2014. Disorders of propionate and methylmalonate metabolism. *In* Beaudet AL, Vogelstein B, Kinzler KW, Antonarakis SE, Ballabio A, Gibson KM, Mitchell G (ed), The online metabolic and molecular bases of inherited disease. The McGraw-Hill Companies, Inc., New York, NY.

78. Charles TC, Cai GQ, Aneja P 1997. Megaplasmid and chromosomal loci for the PHB degradation pathway in *Rhizobium* (*Sinorhizobium*) *meliloti*. Genetics 146:1211–1220.

79. Hunaiti AA, Kolattukudy PE. 1984. Source of methylmalonyl-coenzyme A for erythromycin synthesis: methylmalonyl-coenzyme A mutase from *Streptomyces erythreus*. Antimicrob Agents Chemother 25:173–178. https://doi.org/10.1128/aac.25.2.173.

80. Han Y, Hawkins AS, Adams MW, Kelly RM. 2012. Epimerase (Msed_0639) and mutase (Msed_0638 and Msed_2055) convert (*S*)-methylmalonyl-coenzyme A (CoA) to succinyl-CoA in the *Metallosphaera sedula* 3-hydroxypropionate/4-hydroxybutyrate cycle. Appl Environ Microbiol 78:6194–6202. https://doi.org/10.1128/AEM.01312-12.

81. Aldor IS, Kim SW, Prather KL, Keasling JD. 2002. Metabolic engineering of a novel propionate-independent pathway for the production of poly(3-hydroxybutyrate-*co*-3-hydroxyvalerate) in recombinant *Salmonella enterica* serovar Typhimurium. Appl Environ Microbiol 68:3848–3854. https://doi.org/10.1128/aem.68.8.3848-3854.2002.

82. Gonzalez-Garcia RA, McCubbin T, Wille A, Plan M, Nielsen LK, Marcellin E. 2017. Awakening sleeping beauty: production of propionic acid in *Escherichia coli* through the *sbm* operon requires the activity of a methylmalonyl-CoA epimerase. Microb Cell Fact 16:121. https://doi.org/10.1186/s12934-017-0735-4.

83. Gross F, Ring MW, Perlova O, Fu J, Schneider S, Gerth K, Kuhlmann S, Stewart AF, Zhang Y, Muller R. 2006. Metabolic engineering of *Pseudomonas putida* for methylmalonyl-CoA biosynthesis to enable complex heterologous secondary metabolite formation. Chem Biol 13:1253–1264. https://doi.org/10.1016/j.chembiol.2006.09.014.

84. Reeves AR, Brikun IA, Cernota WH, Leach BI, Gonzalez MC, Weber JM. 2007. Engineering of the methylmalonyl-CoA metabolite node of *Saccharopolyspora erythraea* for increased erythromycin production. Metab Eng 9:293–303. https://doi.org/10.1016/j.ymben.2007.02.001.

85. Dayem LC, Carney JR, Santi DV, Pfeifer BA, Khosla C, Kealey JT. 2002. Metabolic engineering of a methylmalonyl-CoA mutase-epimerase pathway for complex polyketide biosynthesis in *Escherichia coli*. Biochemistry 41:5193–5201. https://doi.org/10.1021/bi015593k.

86. Li J, Zhu X, Chen J, Zhao D, Zhang X, Bi C. 2017. Construction of a novel anaerobic pathway in *Escherichia coli* for propionate production. BMC Biotechnol 17:38–38. https://doi.org/10.1186/s12896-017-0354-5.

87. Srirangan K, Akawi L, Liu X, Westbrook A, Blondeel EJ, Aucoin MG, Moo-Young M, Chou CP. 2013. Manipulating the sleeping beauty mutase operon for the production of 1-propanol in engineered *Escherichia coli*. Biotechnol Biofuels 6:139. https://doi.org/10.1186/1754-6834-6-139.

88. Akawi L, Srirangan K, Liu X, Moo-Young M, Perry Chou C. 2015. Engineering *Escherichia coli* for high-level production of propionate. J Ind Microbiol Biotechnol 42:1057–1072. https://doi.org/10.1007/s10295-015-1627-4.

89. Chowdhury S, Banerjee R. 1999. Role of the dimethylbenzimidazole tail in the reaction catalyzed by coenzyme B_{12}-dependent methylmalonyl-CoA mutase. Biochemistry 38:15287–15294. https://doi.org/10.1021/bi9914762.

90. De Hertogh AA, Mayeux PA, Evans HJ. 1964. The relationship of cobalt requirement to propionate metabolism in *Rhizobium*. J Biol Chem 239:2446–2453.

91. Charles TC, Aneja P 1999. Methylmalonyl-CoA mutase encoding gene of *Sinorhizobium meliloti*. Gene 226:121–127. https://doi.org/10.1016/s0378-1119(98)00555-1.

92. Miyamoto E, Watanabe F, Charles TC, Yamaji R, Inui H, Nakano Y. 2003. Purification and characterization of homodimeric methylmalonyl-CoA mutase from *Sinorhizobium meliloti*. Arch Microbiol 180:151–154. https://doi.org/10.1007/s00203-003-0570-3.

93. Haller T, Buckel T, Rétey J, Gerlt JA. 2000. Discovering new enzymes and metabolic pathways: conversion of succinate to propionate by *Escherichia coli*. Biochemistry 39:4622–4629. https://doi.org/10.1021/bi992888d.

94. Kliewer M, Evans HJ. 1963. Identification of cobamide coenzyme in nodules of symbionts & isolation of the B_{12} coenzyme from *Rhizobium meliloti*. Plant Physiol 38:55–59. https://doi.org/10.1104/pp.38.1.55.

95. Hazra AB, Han AW, Mehta AP, Mok KC, Osadchiy V, Begley TP, Taga ME. 2015. Anaerobic biosynthesis of the lower ligand of vitamin B_{12}. Proc Natl Acad Sci U S A 112:10792–10797. https://doi.org/10.1073/pnas.1509132112.

96. Crofts TS, Seth EC, Hazra AB, Taga ME. 2013. Cobamide structure depends on both lower ligand availability and CobT substrate specificity. Chem Biol 20:1265–1274. https://doi.org/10.1016/j.chembiol.2013.08.006.

97. Froese DS, Kochan G, Muniz JR, Wu X, Gileadi C, Ugochukwu E, Krzysztofinska E, Gravel RA, Oppermann U, Yue WW. 2010. Structures of the human GTPase MMAA and vitamin B_{12}-dependent methylmalonyl-CoA mutase and insight into their complex formation. J Biol Chem 285:38204–38213. https://doi.org/10.1074/jbc.M110.177717.

98. Miyamoto E, Tanioka Y, Nishizawa-Yokoi A, Yabuta Y, Ohnishi K, Misono H, Shigeoka S, Nakano Y, Watanabe F. 2010. Characterization of methylmalonyl-CoA mutase involved in the propionate photoassimilation of *Euglena gracilis* Z. Arch Microbiol 192:437–446. https://doi.org/10.1007/s00203-010-0572-x.

99. Miyamoto E, Watanabe F, Yamaji R, Inui H, Sato K, Nakano Y. 2002. Purification and characterization of methylmalonyl-CoA mutase from a methanol-utilizing bacterium, *Methylobacterium extorquens* NR-1. J Nutr Sci Vitaminol (Tokyo) 48:242–246. https://doi.org/10.3177/jnsv.48.242.

100. Birch A, Leiser A, Robinson JA. 1993. Cloning, sequencing, and expression of the gene encoding methylmalonyl-coenzyme A mutase from *Streptomyces cinnamonensis*. J Bacteriol 175:3511–3519. https://doi.org/10.1128/jb.175.11.3511-3519.1993.

101. Zhang W, Yang L, Jiang W, Zhao G, Yang Y, Chiao J. 1999. Molecular analysis and heterologous expression of the gene encoding methylmalonyl-coenzyme A mutase from rifamycin SV-producing strain *Amycolatopsis mediterranei* U32. Appl Biochem Biotechnol 82:209–225. https://doi.org/10.1385/ABAB:82:3:209.

102. Yabuta Y, Kamei Y, Bito T, Arima J, Yoneda K, Sakuraba H, Ohshima T, Nakano Y, Watanabe F. 2015. Functional and structural characteristics of methylmalonyl-CoA mutase from *Pyrococcus horikoshii*. Biosci Biotechnol Biochem 79:710–717. https://doi.org/10.1080/09168451.2014.993353.

103. Chowdhury S, Thomas MG, Escalante-Semerena JC, Banerjee R. 2001. The coenzyme B_{12} analog 5′-deoxyadenosylcobinamide-GDP supports catalysis by methylmalonyl-CoA mutase in the absence of trans-ligand coordination. J Biol Chem 276:1015–1019. https://doi.org/10.1074/jbc.M006842200.

104. Kanehisa M, Goto S. 2000. KEGG: Kyoto encyclopedia of genes and genomes. Nucleic Acids Res 28:27–30. https://doi.org/10.1093/nar/28.1.27.

105. Schubert T, von Reuß SH, Kunze C, Paetz C, Kruse S, Brand-Schön P, Nelly AM, Nüske J, Diekert G. 2019. Guided cobamide biosynthesis for heterologous production of reductive dehalogenases. Microb Biotechnol 12:346–359. https://doi.org/10.1111/1751-7915.13339.

106. Borths EL, Poolman B, Hvorup RN, Locher KP, Rees DC. 2005. In vitro functional characterization of BtuCD-F, the *Escherichia coli* ABC transporter for vitamin B_{12} uptake. Biochemistry 44:16301–16309. https://doi.org/10.1021/bi0513103.

107. Heller K, Mann BJ, Kadner RJ. 1985. Cloning and expression of the gene

for the vitamin B_{12} receptor protein in the outer membrane of *Escherichia coli*. J Bacteriol 161:896–903.

108. Hazra AB, Tran JL, Crofts TS, Taga ME. 2013. Analysis of substrate specificity in CobT homologs reveals widespread preference for DMB, the lower axial ligand of vitamin B_{12}. Chem Biol 20:1275–1285. https://doi.org/10.1016/j.chembiol.2013.08.007.

109. Mukherjee S, Das Mandal S, Gupta N, Drory-Retwitzer M, Barash D, Sengupta S. 2019. RiboD: a comprehensive database for prokaryotic riboswitches. Bioinformatics https://doi.org/10.1093/bioinformatics/btz093.

110. Nahvi A, Barrick JE, Breaker RR. 2004. Coenzyme B_{12} riboswitches are widespread genetic control elements in prokaryotes. Nucleic Acids Res 32:143–150. https://doi.org/10.1093/nar/gkh167.

111. Widner FJ, Lawrence AD, Deery E, Heldt D, Frank S, Gruber K, Wurst K, Warren MJ, Krautler B. 2016. Total synthesis, structure, and biological activity of adenosylrhodibalamin, the non-natural rhodium homologue of coenzyme B_{12}. Angew Chem Int Ed Engl 55:11281–11286. https://doi.org/10.1002/anie.201603738.

112. Calafat AM, Taoka S, Puckett JM, Semerad C, Yan H, Luo L, Chen H, Banerjee R, Marzilli LG. 1995. Structural and electronic similarity but functional difference in methylmalonyl-CoA mutase between coenzyme B_{12} and the analog 2′,5′-dideoxyadenosylcobalamin. Biochemistry 34:14125–14130. https://doi.org/10.1021/bi00043a017.

113. Fukuoka M, Nakanishi Y, Hannak RB, Krautler B, Toraya T. 2005. Homoadenosylcobalamins as probes for exploring the active sites of coenzyme B_{12}-dependent diol dehydratase and ethanolamine ammonia-lyase. FEBS J 272:4787–4796. https://doi.org/10.1111/j.1742-4658.2005.04892.x.

114. Santos JA, Rempel S, Mous STM, Pereira CT, ter Beek J, de Gier J-W, Guskov A, Slotboom DJ. 2018. Functional and structural characterization of an ECF-type ABC transporter for vitamin B_{12}. Elife 7:e35828. https://doi.org/10.7554/eLife.35828.

115. Rodionov DA, Hebbeln P, Eudes A, ter Beek J, Rodionova IA, Erkens GB, Slotboom DJ, Gelfand MS, Osterman AL, Hanson AD, Eitinger T. 2009. A novel class of modular transporters for vitamins in prokaryotes. J Bacteriol 191:42–51. https://doi.org/10.1128/JB.01208-08.

116. Johnson CL, Pechonick E, Park SD, Havemann GD, Leal NA, Bobik TA. 2001. Functional genomic, biochemical, and genetic characterization of the *Salmonella pduO* gene, an ATP:cob(I)alamin adenosyltransferase gene. J Bacteriol 183:1577–1584. https://doi.org/10.1128/JB.183.5.1577-1584.2001.

117. Escalante-Semerena JC, Suh SJ, Roth JR. 1990. *cobA* function is required for both de novo cobalamin biosynthesis and assimilation of exogenous corrinoids in *Salmonella typhimurium*. J Bacteriol 172:273–280. https://doi.org/10.1128/jb.172.1.273-280.1990.

118. Abreu NA, Taga ME. 2016. Decoding molecular interactions in microbial communities. FEMS Microbiol Rev 40:648–663. https://doi.org/10.1093/femsre/fuw019.

119. Degnan PH, Taga ME, Goodman AL. 2014. Vitamin B_{12} as a modulator of gut microbial ecology. Cell Metab 20:769–778. https://doi.org/10.1016/j.cmet.2014.10.002.

120. Seth EC, Taga ME. 2014. Nutrient cross-feeding in the microbial world. Front Microbiol 5:350. https://doi.org/10.3389/fmicb.2014.00350.

121. Yan J, Ritalahti KM, Wagner DD, Loffler FE. 2012. Unexpected specificity of interspecies cobamide transfer from *Geobacter* spp. to organohalide-respiring *Dehalococcoides mccartyi* strains. Appl Environ Microbiol 78:6630–6636. https://doi.org/10.1128/AEM.01535-12.

122. Ma AT, Beld J, Brahamsha B. 2017. An amoeba grazer of cyanobacteria requires cobalamin produced by heterotrophic bacteria. Appl Environ Microbiol 83:e00035-17. https://doi.org/10.1128/AEM.00035-17.

123. Belzer C, Chia LW, Aalvink S, Chamlagain B, Piironen V, Knol J, de Vos WM. 2017. Microbial metabolic networks at the mucus layer lead to diet-independent butyrate and vitamin B_{12} production by intestinal symbionts. mBio 8:e00770-17. https://doi.org/10.1128/mBio.00770-17.

124. Heal KR, Qin W, Ribalet F, Bertagnolli AD, Coyote-Maestas W, Hmelo LR, Moffett JW, Devol AH, Armbrust EV, Stahl DA, Ingalls AE. 2017. Two distinct pools of B_{12} analogs reveal community interdependencies in the ocean. Proc Natl Acad Sci U S A 114:364–369. https://doi.org/10.1073/pnas.1608462114.

125. Fortier A, Grosdidier A, Hernandez C, Baratin D, Kuznetsov D, de Castro E, Gasteiger E, Csardi G, Rossier G, Stockinger H, Xenarios I, Mostaguir K, Arnold K, Jonnalagedda M, Redaschi N, Artimo P, Liechti R, Moretti S,

Duvaud S, Ioannidis V, Flegel V. 2012. ExPASy: SIB bioinformatics resource portal. Nucleic Acids Res 40:W597–W603. https://doi.org/10.1093/nar/gks400.

126. Crosby HA, Rank KC, Rayment I, Escalante-Semerena JC. 2012. Structure-guided expansion of the substrate range of methylmalonyl coenzyme A synthetase (MatB) of *Rhodopseudomonas palustris*. Appl Environ Microbiol 78:6619–6629. https://doi.org/10.1128/AEM.01733-12.

127. Hoffmann B, Oberhuber M, Stupperich E, Bothe H, Buckel W, Konrat R, Kräutler B. 2000. Native corrinoids from *Clostridium cochlearium* are adeninylcobamides: spectroscopic analysis and identification of pseudovitamin B_{12} and factor A. J Bacteriol 182:4773–4782. https://doi.org/10.1128/jb.182.17.4773-4782.2000.

128. Crofts TS, Hazra AB, Tran JL, Sokolovskaya OM, Osadchiy V, Ad O, Pelton J, Bauer S, Taga ME. 2014. Regiospecific formation of cobamide isomers is directed by CobT. Biochemistry 53:7805–7815. https://doi.org/10.1021/bi501147d.

129. Kopf J, Deuten KV, Bieganowski R, Friedrich W. 1981. X-ray crystal structure analysis of factor A (2-methyladeninyl-cyanocobamide), a native vitamin B_{12}-analogue. Z Naturforsch C 36:506–515. https://doi.org/10.1515/znc-1981-7-802.

130. Brown KL, Zou X. 1999. Thermolysis of coenzymes B_{12} at physiological temperatures: activation parameters for cobalt-carbon bond homolysis and a quantitative analysis of the perturbation of the homolysis equilibrium by the ribonucleoside triphosphate reductase from *Lactobacillus leichmannii*. J Inorg Biochem 77:185–195. https://doi.org/10.1016/S0162-0134(99)00190-7.

131. Hogenkamp H. 1975. The chemistry of cobalamins and related compounds, p 55. *In* Babior BM (ed), Cobalamin biochemistry and pathophysiology. John Wiley and Sons, Inc, New York, NY.

132. Schneider Z, Stroinski A. 1987. Comprehensive B_{12}: chemistry, biochemistry, nutrition, ecology, medicine. Walter de Gruyter, Berlin, Germany.

133. Stupperich E, Eisinger HJ, Krautler B. 1988. Diversity of corrinoids in acetogenic bacteria. *P*-cresolylcobamide from *Sporomusa ovata*, 5-methoxy-6-methylbenzimidazolylcobamide from *Clostridium formicoaceticum* and vitamin B_{12} from *Acetobacterium woodii*. Eur J Biochem 172:459–464. https://doi.org/10.1111/j.1432-1033.1988.tb13910.x.

134. Warner JR, Copley SD. 2007. Pre-steady-state kinetic studies of the reductive dehalogenation catalyzed by tetrachlorohydroquinone dehalogenase. Biochemistry 46:13211–13222. https://doi.org/10.1021/bi701069n.

135. Guex N, Peitsch MC, Schwede T. 2009. Automated comparative protein structure modeling with SWISS-MODEL and Swiss-PdbViewer: a historical perspective. Electrophoresis 30(Suppl 1):S162–S173. https://doi.org/10.1002/elps.200900140.

136. Schrödinger LLC. 2015. Maestro. Schrödinger LLC, New York, NY.

137. Schrödinger LLC. 2015. MacroModel. Schrödinger LLC, New York, NY.

138. Taoka S, Padmakumar R, Lai MT, Liu HW, Banerjee R. 1994. Inhibition of the human methylmalonyl-CoA mutase by various CoA-esters. J Biol Chem 269:31630–31634.

139. Campbell GR, Taga ME, Mistry K, Lloret J, Anderson PJ, Roth JR, Walker GC. 2006. *Sinorhizobium meliloti bluB* is necessary for production of 5,6-dimethylbenzimidazole, the lower ligand of B_{12}. Proc Natl Acad Sci U S A 103:4634–4639. https://doi.org/10.1073/pnas.0509384103.

140. Banerjee RV, Johnston NL, Sobeski JK, Datta P, Matthews RG. 1989. Cloning and sequence analysis of the *Escherichia coli metH* gene encoding cobalamin-dependent methionine synthase and isolation of a tryptic fragment containing the cobalamin-binding domain. J Biol Chem 264:13888–13895.

141. Sato K, Inukai S, Shimizu S. 1974. Vitamin B_{12}-dependent methionine synthesis in *Rhizobium meliloti*. Biochem Biophys Res Commun 60:723–728. https://doi.org/10.1016/0006-291x(74)90300-3.

142. Cowles JR, Evans HJ, Russell SA. 1969. B_{12} coenzyme-dependent ribonucleotide reductase in *Rhizobium* species and the effects of cobalt deficiency on the activity of the enzyme. J Bacteriol 97:1460–1465.

143. Taga ME, Walker GC. 2010. *Sinorhizobium meliloti* requires a cobalamin-dependent ribonucleotide reductase for symbiosis with its plant host. Mol Plant Microbe Interact 23:1643–1654. https://doi.org/10.1094/MPMI-07-10-0151.

144. Maniatis T, Fritsch EF, Sambrook J. 1989. Molecular cloning: a laboratory manual. Cold Spring Harbor Laboratory Press, Cold Spring Harbor, NY.